WP5
Integration and testing of DSS for coastal flood and extreme weather early warning

Activity 5.3
Pilot action around the Pescara river estuary coastline area

D5.3.1
PAI: pilot action around the Pescara river estuary coastline area

PROJECT AND ACTIVITY DETAILS

Project Acronym	AdriaMORE
Project title	Adriatic DSS exploitation for MOnitoring and Risk management of coastal Extreme weather and flooding
Funding Line	Priority Axis 2, Specific Objective 2.2
Project Partners	LP Abruzzo Region (Italy) P1 Dubrovnik and Neretva Region (Croatia) P2 Meteorological and hydrological service (Croatia) P3 National Research Council (Italy)
Starting date	January 1, 2018
Activity number	5.3
Activity Title	Pilot action around the Pescara river estuary
Work Package	WP5: Integration and testing of DSS for coastal flood and extreme weather early warning
Activity Summary	Activity 5.3, within work package 5, is devoted to test the developed modeling and observation modules on a severe weather event chosen during the pilot action around the Pescara river estuary coastline area.
Deliverable number	5.3.1
Deliverable Summary	This deliverable is aimed at describing the case study of the Italian pilot action by means forecast, observational and transport numerical simulations results
Main Author	Valentina Colaiuda, Federico Falcini, Rossella Ferretti, Giovanni La Forgia and Errico Picciotti
Main Author's organization	CETEMPS and CNR-ISMAR (PP3)
Other Author's	Stefano Barbieri, Alessandro Coluccelli, Raffaele Corrado, Saverio Di Fabio, Guglielmo Lacorata, Annalina Lombardi and Barbara Tomassetti
Data of issue	November, 30 2019
Total Number of pages	57
Distribution list	Italy-Croatia CBC Programme, AdriaMORE partners

This document has been produced with the contribution of the EU co-financing and the Interreg Italy-Croatia CBC Programme. The content reflects the author's views; the Programme authorities are not liable for any use that may be made of the information contained therein.

Table of contents

Introduction

This report is aimed at describing the case study as well as forecast and observational results during the Pilot Action along Italian coastlines (called PAI) devoted to the Abruzzo region near the estuary of the Pescara river.

Among the Intensive Observation Periods (IOPs) collected during the PAI Campaign we selected and described in the following one relevant case study that affected the Pescara coastal area happened between 12rd and 14th May 2019 and that had the greatest effects on the last day when a discharge peak involved the area of Pescara. This case study has been chosen because of the density of observations but also for their severity and the hydro-geological/economic effects on the territory involved in. The event has been analyzed from both observing and modeling points of view and the results are shown in following paragraphs.

The PAI preparations activities have been started since the beginning of the project by completing successfully the WP3 and WP4.

In the framework of WP3 activities a weather radar composite software able to ingest and process data from systems with different features was developed and a WEB interface has been arranged where the instantaneous rainfall estimates for the Croatian and Italian composites are displayed in real-time.

In the framework of WP4 activities was implemented a coupled model, containing both a meteorological and a wave model, respectively called WRF and SWAN, adapted and calibrated over the target basin on a case study-basis. Moreover, was operationally implemented the CHyM hydrological model with *waveheight* module able to read sea level measurements in input, to modify the friction of the river flow in the river outlet, enhancing the coastal flood prediction capability.

Finally in WP4, numerical model simulations of transport and dispersion in the Adriatic Sea basin were developed. An established modelling software was set up in order to simulate Lagrangian trajectories on the sea surface adapted for large-scale circulation fields whereas an innovative Lagrangian model for the unresolved sub-grid scale motions, takes into account small-scale turbulent dispersion.

In the activities related to this report all outputs produced in the previous WP3 and WP4 were interconnected in a coherent way in order to set up an early hydro-meteo-marine forecast and observation system integrated in the existing MyDewetra platform. All outputs has been tested on the identified case study in order to verify their capability to identify critical situation over the Pescara river estuary, for this purpose the available rain gauges, satellite and lightning data were used through MyDewetra platform.

These activities have been carried out by CETEMPS and CNR-ISMAR, the latter as partner of AdriaMORE project. It is worth recalling that the Centre of Excellence (CETEMPS) of the University of L'Aquila is a joint effort of the Dept. of Physics and the Dept. of Electrical Engineering, funded by the Ministry of Education and University of Italy starting from 2001. The research activity concerns mainly remote sensing, atmospheric physics, meteorology and hydrology. CETEMPS has a contractual agreement with the LP Region Abruzzo to support the accomplishment of some technical activities of AdriaMORE project.

The present document is, then, organized as follows:
Paragraph 1 contains a brief description of the estuary of Pescara river area;
Paragraph 2 is dedicated to a description of the major hazards that can affect the Abruzzi coast;
Paragraph 3 is devoted to the description of the PAI case study;
Paragraph 4 is devoted to the meteorological model results of the storm surge of 14th May 2019;
Paragraph 5 is devoted to the results of the CHyM forecast applied to the 14th May 2019 discharge peak;
Paragraph 6 is devoted to the observation analysis using radar, rain gauges, satellite and lightning data;
Paragraph 7 is devoted at evaluating of Eulerian and Lagrangian observables to meteo-hydrological forcings and to the presence of artificial barriers in the harbor by means of numerical simulations.

1. Description of the estuary of the Pescara river

The Pescara river is the second largest river in Italy that flows into the Adriatic, after the river Po. The total length from the Aterno springs to the sea is 145 km and crosses the Abruzzo from west to east (**figures 1.1 and 1.2**). The Pescara river comes from the homonymous source upstream of Popoli and after a short journey, at the confluence of the Aterno and Sagittario rivers, it receives its waters and takes the name of Pescara river. Before flowing into the Adriatic, along the way, receives the waters of various tributaries: Swan, Garden, Nora, Tirino and Orta. The mouth, located in the channel port, is located in the town of the city of Pescara.

Since 1986, the entire area of the springs of Pescara, in Popoli, is a Regional Natural Reserve. The Reserve protects the vast mirror of transparent water created by the numerous springs and underwater pools. The waters come directly from Campo Imperatore, the vast plateau of the Gran Sasso, after a journey lasting about 30 days, and are concentrated in the area of Capo Pescara, creating a unique spectacle. The Reserve can be visited all year round.

Figure 1.1: map of the river

Figure 1.2: on the left the Pescara springs; on the right the Pescara river around Popoli town

Pescara is the largest city of Abruzzi region, and among the main commercial and tourist centers along the Adriatic coast. Its sandy beaches extend for over 20 uninterrupted km, and the areas in the hinterland underwent a remarkable development, so that presently there exist one wide conurbation, including nearby municipalities as Montesilvano, Chieti, Francavilla, Città Sant'Angelo, Spoltore, where over 400,000 people are concentrated (one third of the whole Abruzzi population).

2. Major hazards that affect the Pescara river area

The health of estuaries is threatened by coastal development, declining water quality and loss of habitat for native species. Estuaries are impacted by pressures from human activities as well as natural events such as storms and floods. They are complex, dynamic and relatively fragile environments. Estuaries are particularly sensitive to inappropriate catchment development, increased levels of sediment and nutrients and the degree of tidal flushing – the exchange of fresh water and ocean water.

Estuary management committees, councils, agencies and the community have identified several issues affecting estuaries including:

- declining estuarine water and sediment quality;
- degradation and loss of estuarine habitats;
- unsustainable coastal development and use of estuarine resources.

The estuary of the Pescara river is an area highly urbanized and prone to coastal flooding as well as to extreme weather. The major hazards are represented by heavy precipitation events along the Aterno-Pescara river that typically cause a major river flow which may cause river flooding within the city of Pescara, problem of boats re-entering toward the port of Pescara and finally a runoff of materials along the river making the sea water around the port more turbid and eventually polluted (see in the **figure 2.1** an image of this phenomenon).

Figure 2.1: an image of the Pescara river in which it exceeds the level of early warning

3. Case study description

The chosen case study over the Pescara coastal area happened between 12rd and 14th May 2019, when a discharge peak involved the Pescara coastal area do to a combination of moderate-heavy precipitation and sea level raise. The description and meteorological and hydrological forecast analysis are focused on the last two days when the greatest effects have occurred in terms of precipitation (13 May) and storm surges (14 May).

3.1 Synoptic description

On May 13rd a deep through is was extending its axis from the Scandinavian Peninsula down to the North-Africa coastal areas. A cut-off low was moving in South-East direction along the Italian Peninsula, causing a cyclonic circulation over central Italy with cold airmass flow from Siberia. The Abruzzo region was hit by E-NE circulation of the return-branch originating from the cut-off vortex, which was located between two high pressure areas: a ridge extending its axis from the Iberian Peninsula to Britain and another area affecting the eastern Europe. For this reason, the low pressure over the Mediterranean are was particularly persistent (**figure 3.1.1**). The airmass RGB image in **figure 3.1.2** shows the presence of thick clouds over Central Italy together with cold air coming from northern latitudes. The reddish airmass flow shows a dry-air channel over the Tyrrhenian Sea due to a potential vorticity positive anomaly, that can be also seen from the water vapor channel satellite image and vorticity at 300 hPa.

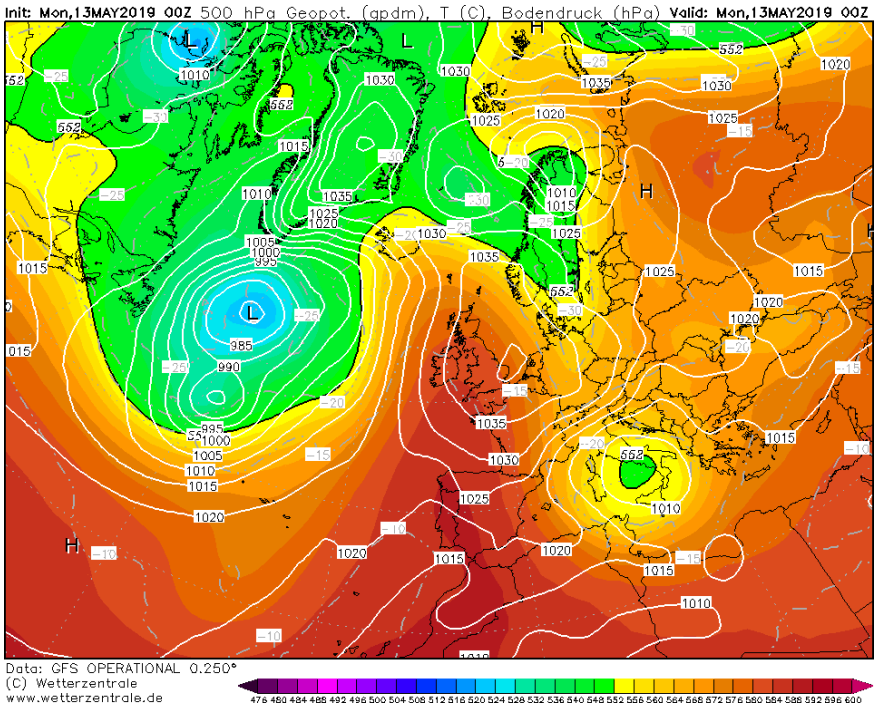

Figure 3.1.1: 500 hPa Geopotential height (colour shades) and atmospheric pressure a.s.l. (isolines) on May 13th over Europe

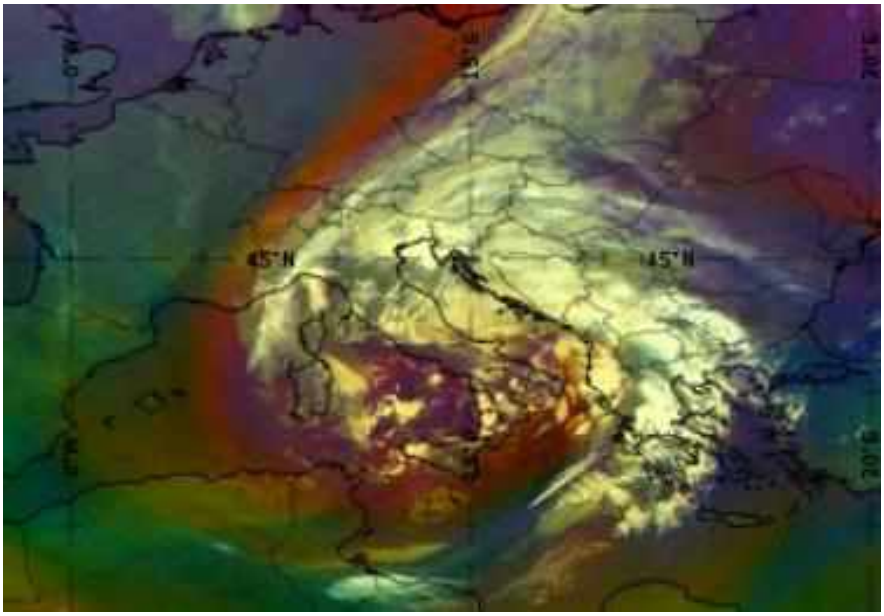

a) Airmass RGB satellite composite on May 13th

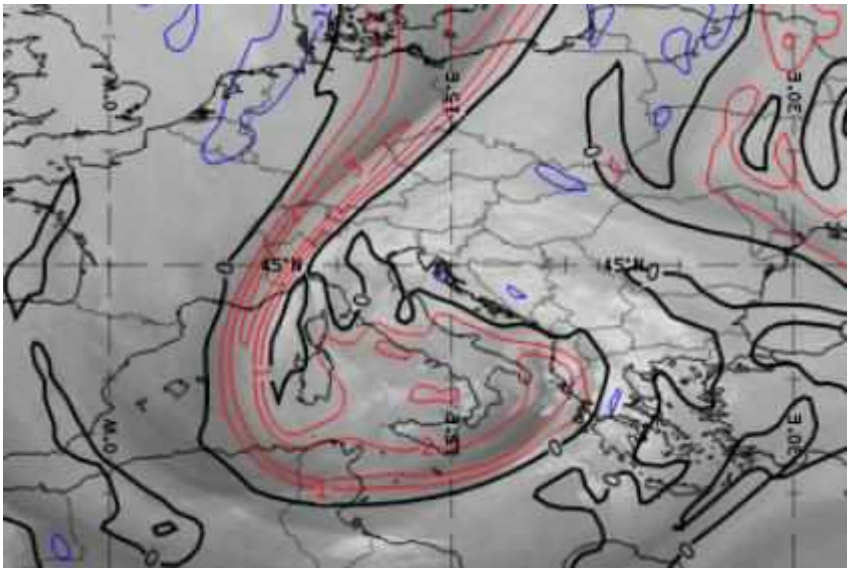

b) Water vapor channel and potential vorticity anomalies (isolines) on May 13th

Figure 3.1.2: satellite images detected on May 13th, 2019

On May 14th a orographic convection is intensified over Apennine's ridges, while the cyclogenesis progressively filled, moving toward Sothern Italy (**figure 3.1.3**).

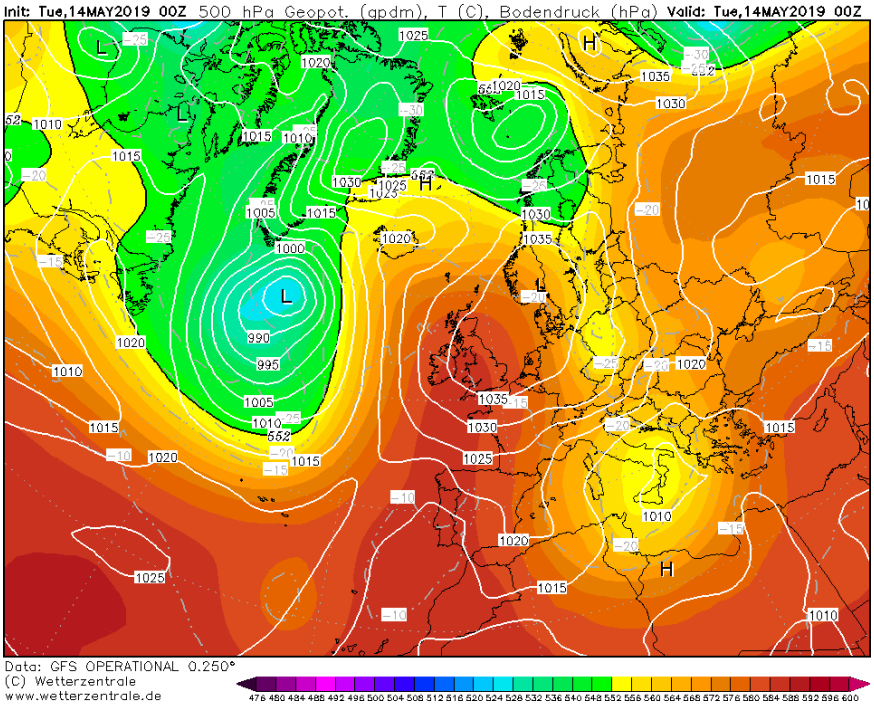

Figure 3.1.3: 500 hPa Geopotential height (colour shades) and atmospheric pressure a.s.l. (isolines) on May 14th over Europe

3.2 Effects at ground

Maps shown in **figure 3.2.1** reveals as the maximum precipitation occurred on May 13th. Rainfall peaks were affecting Apennine's ridge and piedmont eastern areas during the first day of the event, while weaker maxima moved over coastal areas in the following day. The discharge peak arrived in the Pescara river mouth on May 14th afternoon: its transition was registered over the last hydrometric station "Pescara S. Teresa" at 16:00 LT (**figure 3.2.2**).

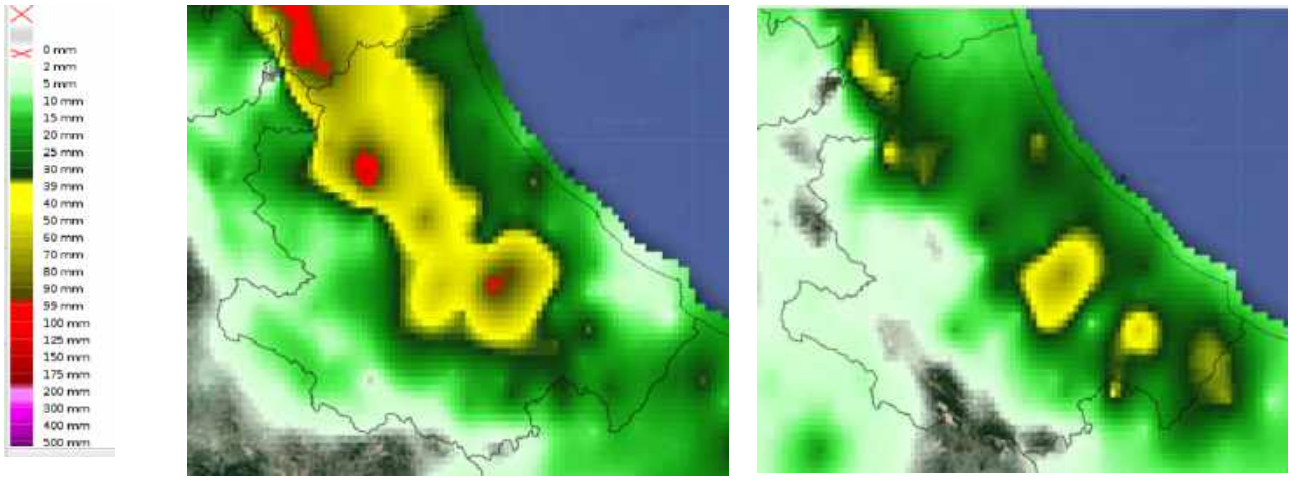

a) 24 accumulated rainfall over Abruzzo region on May 13rd 2019

b) 24 h accumulated rainfall over Abruzzo Region on May 14th 2019

Figure 3.2.1: precipitation accumulated during the event

Figure 3.2.2: hydrometric level timeseries during the event, observed at Pescara S. Teresa station

The sea level timeseries detected by the Pescara seaport station is shown in **figure 3.2.3**. A strong ventilation from E-NE was affecting the Adriatic coast, causing storm surge (**figure 3.2.4**) whose effect can be seen in **figure 3.2.5**.

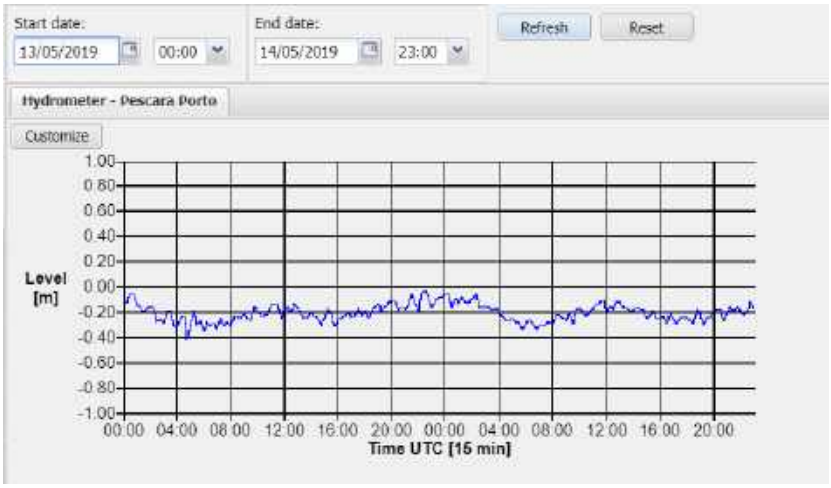

Figure 3.2.3: sea level timeseries detected by the Pescara seaport station

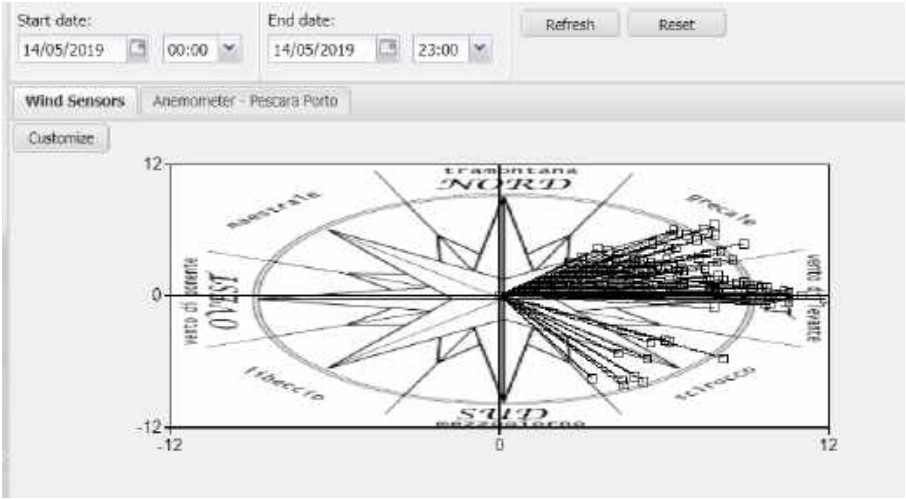

Figure 3.2.4: wind direction and intensity observed in the Pescara harbor station

Figure 3.2.5: an image of the coastal storm that affected the Abruzzi region

4. Meteorological forecast

Following, the results obtained by the coupled system WRF-SWAN on the case study analysed (details of the two models are described in the Deliverable 4.3.1).

In **figure 4.1** there are two images of the 6-hrs accumulated precipitations respectively at 00UTC (on the left) and at 06UTC (on the right) of the 14 May 2019. It can be noticed that the major rainfall (around 20-30 mm/6h) are localized along the Apennines ridge and in the south-eastern part of the Abruzzi region, including the coastal area.

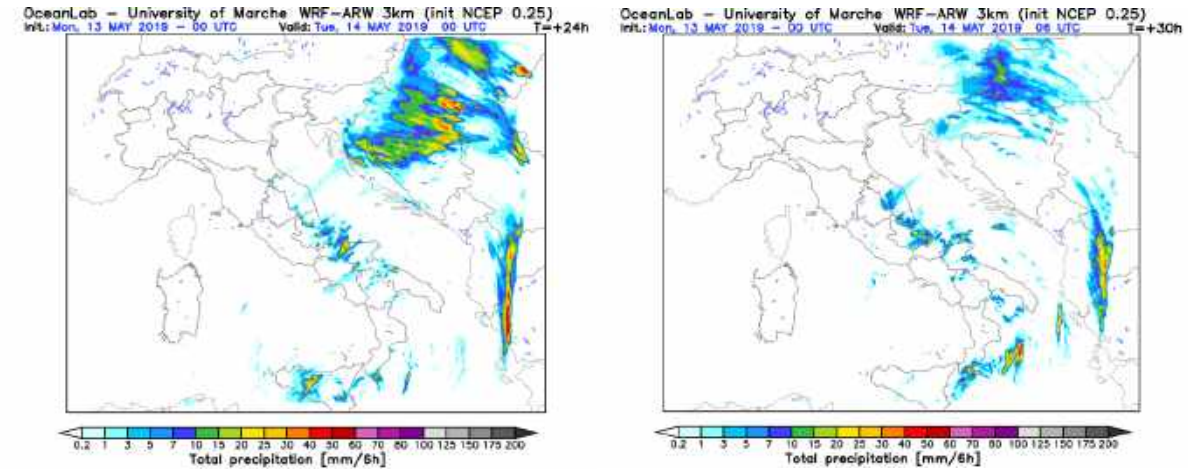

Figure 4.1: two images of the 6-hrs accumulated precipitations of the coupled WRF-SWAN model, respectively @00UTC (on the left) and @06UTC (on the right) of the 14 May 2019.

If we analyze the wind speed field, the two images of **figure 4.2** clearly show both fresh and strong winds from north-east respectively at 00UTC (on the left) and at 06UTC (on the right) of the 14 May 2019, that impact all the coastal area.

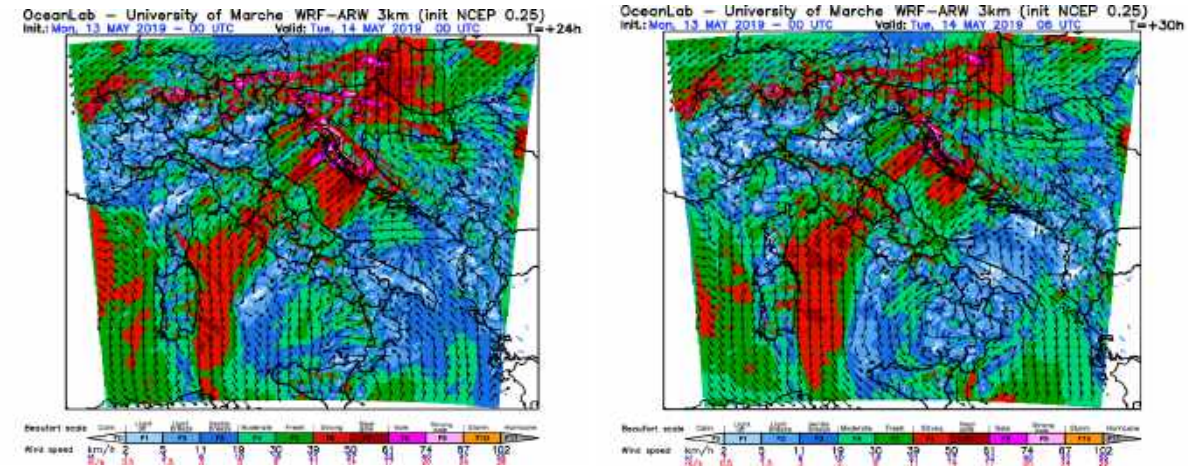

Figure 4.2: two images of the wind speed of the coupled WRF-SWAN model, respectively @00UTC (on the left) and @06UTC (on the right) of the 14 May 2019.

Moreover, from the coupled system WRF-SWAN it is possible to obtain some several sea products at a spatial resolution of 1km, such as the significant wave height and direction, the surface currents and the sea surface height.

In **figure 4.3** there are two images of the significant wave height and direction respectively at 00UTC (on the left) and at 06UTC (on the right) of the 14 May 2019. As you can see, above all at midnight, the Middle Adriatic had a significant wave height between 1.5 and 2.75 meters with a wave direction from north-east impacting the coasts.

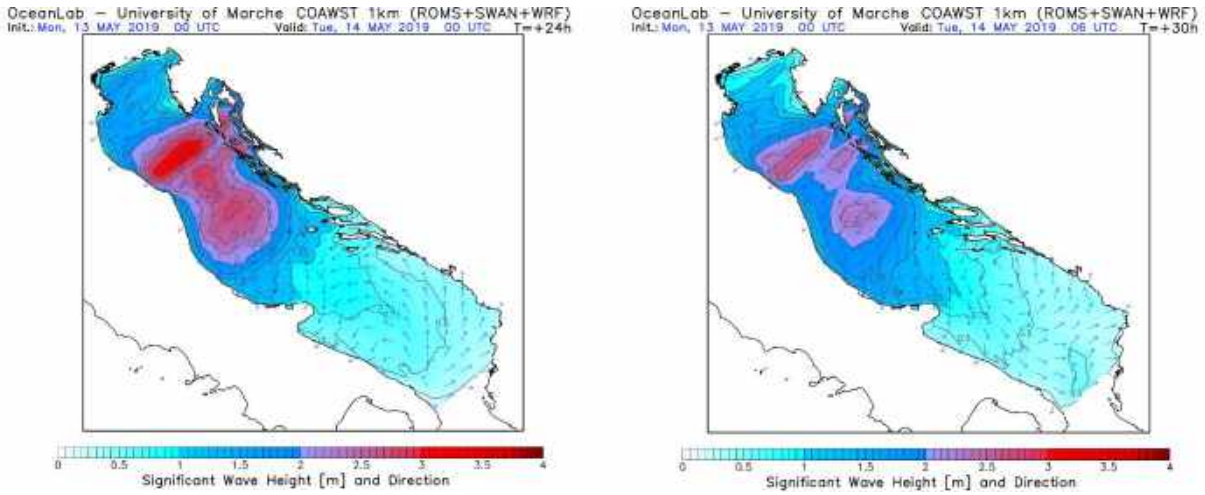

Figure 4.3: two images of the significant wave height and direction of the coupled WRF-SWAN model, respectively @00UTC (on the left) and @06UTC (on the right) of the 14 May 2019.

Concerning the sea surface currents they reached 0.8 m/s (red colour) along the coasts of Abruzzi region, as well as along the Balkans Coasts and the coasts of Puglia region (**figure 4.4**).

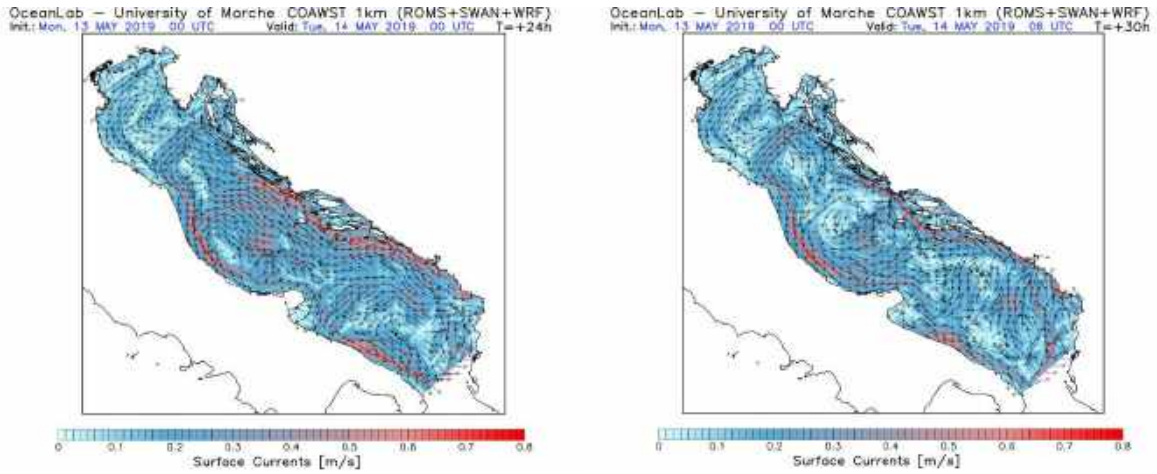

Figure 4.4: two images of the surface currents of the coupled WRF-SWAN model, respectively @00UTC (on the left) and @06UTC (on the right) of the 14 May 2019.

To conclude, we can also take a look at **figure 4.5** showing the sea surface height that, in agreement with the wave height and direction, is more significant at midnight reaching a value of 0.16 meters along the southern coast of Abruzzi.

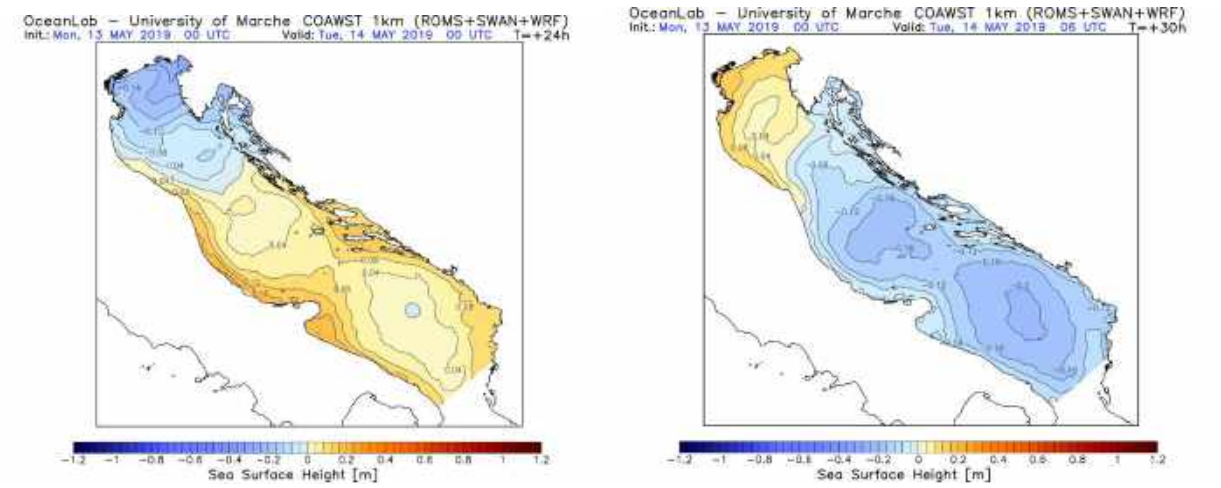

Figure 4.5: two images of the sea surface height of the coupled WRF-SWAN model, respectively @00UTC (on the left) and @06UTC (on the right) of the 14 May 2019.

5. Hydrological forecast

CHyM hydrological new modules have been tested on the identified case study in order to verify its capability to identify critical stress situation over the Pescara river estuary.

The hydrological forecast was issued the day before the event (on May 13th), resulting from a CHyM hydrological simulation initialized with 5 days observed precipitation from the Abruzzo Region rain gauges network. The meteorological forecast was provided from the WRF simulation for the following 72 hours. The forecasted rainfall fields from the WRF model has been interpolated over the 270 m CHyM grid, and is compared to the observed rainfall field, in **figure 5.1**. The forecasted precipitation distribution is quite similar to the observed pattern, obtained by spatializing rain gauges observed data. The WRF forecast moves the precipitation in the eastern piedmont areas, while some maxima are present over the coastal areas. The precipitation amount is slightly overestimated by the meteorological forecast, however, some data from the rain gauges network is missing due to a power cut during the event.

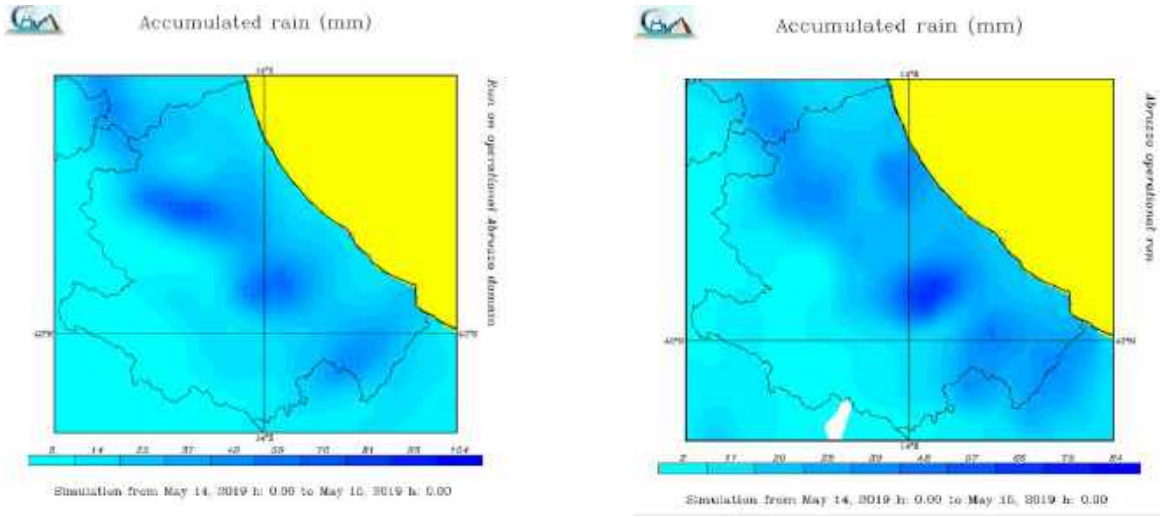

a) WRF forecasted 24h accumulated precipitation on May 14th 2019

b) observed 24h accumulated precipitation on May 14th 2019

Figure 5.1: accumulated precipitation on May 14th 2019

The obtained BDD 24h stress index map on **figure 5.2** are related to the forecasted precipitation amount (figure 5.2, a) and observed precipitation amount used as reference (figure 5.2, b). The stress index over the final path of the Pescara river has the same moderate values in both simulations initialized with the meteorological forecast and observed precipitation, respectively. Some overestimation of the forecast is given over other basins, in the northern part of the region.

The forecasted stress degree exceeded the yellow threshold: we consider this colour-code appropriate for the occurred hydrological event, since the issued hydrogeological criticality bulletin issued on May 14th 2019 reported an orange warning state (**figure 5.3**).

A picture of the Pescara river mouth (the canal port) on May 14th 2019 morning is shown in **figure 5.4.**

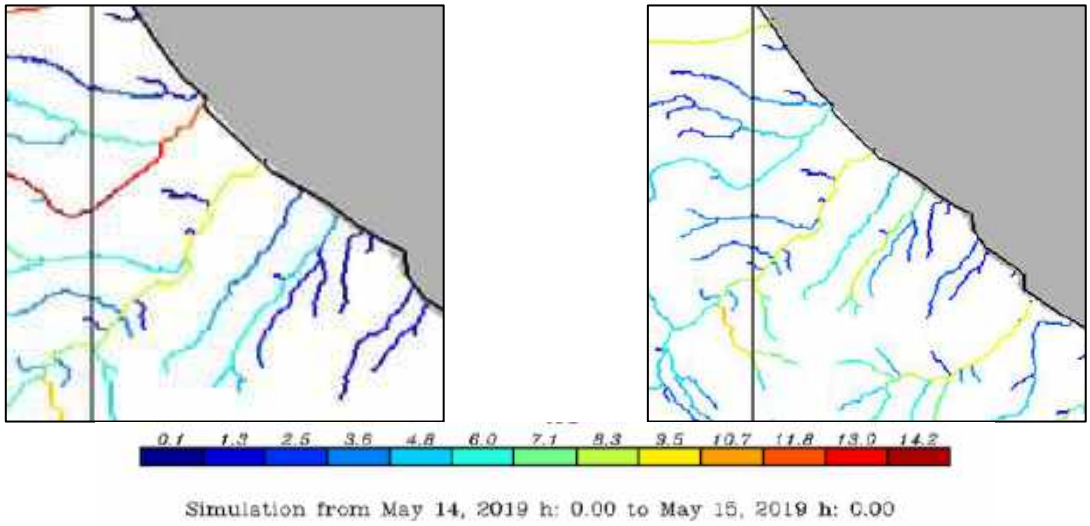

a) BDD stress index in 24h, with the CHyM-WRF forecast

b) BDD stress index in 24h, with the CHyM-OBS forecast

Figure 5.2: BDD stress index maps for 14th May 2019

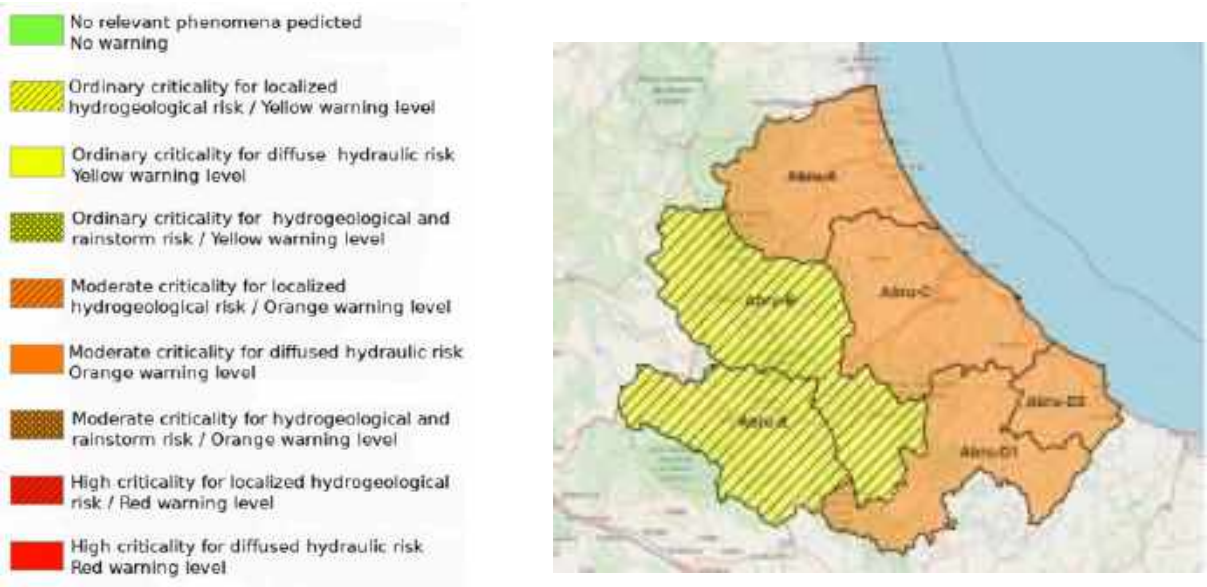

Figure 5.3: criticality bulletin issued by the Abruzzo Region Functional Centre on May 14th 2019

Figure 5.4: picture of the Pescara river mouth (the canal port) on May 14th 2019 morning

6. Observations

Radar, rain gauges, satellite and lightning data were available and visualized by arranged web site and by MyDewetra platform. In the following, the most relevant time frame for the observed data during the whole event happened between 12rd and 14th May 2019 are provided.

6.1 Weather radars network

Weather radars (see **figure 6.1.1**) are ideally suited to provide remotely sensed data of the state of the atmosphere over a wide geographic area. The data provided by weather radars are often used for the near real-time forecasting of weather events by meteorologists, but can also be used to initialize numerical weather predictions and hydrological models. Given the wide uses of data from weather radar, it is not surprising that there has been considerable investment in the development and operation of these instruments worldwide. Networks of radars cover much of the inhabited regions of North America and Europe, providing updated views for severe weather detection and mesoscale flood forecasting. Nonetheless measurements made by weather radars contain a tremendous amount of information, yet considerable effort must be made to extract out scientifically and operationally meaningful products. Processing, correcting and analysing weather radar data covers a wide range of computational disciplines and fields. Given the wide scope of information that weather radars can provide, having flexible and extendable software to process their data is key.

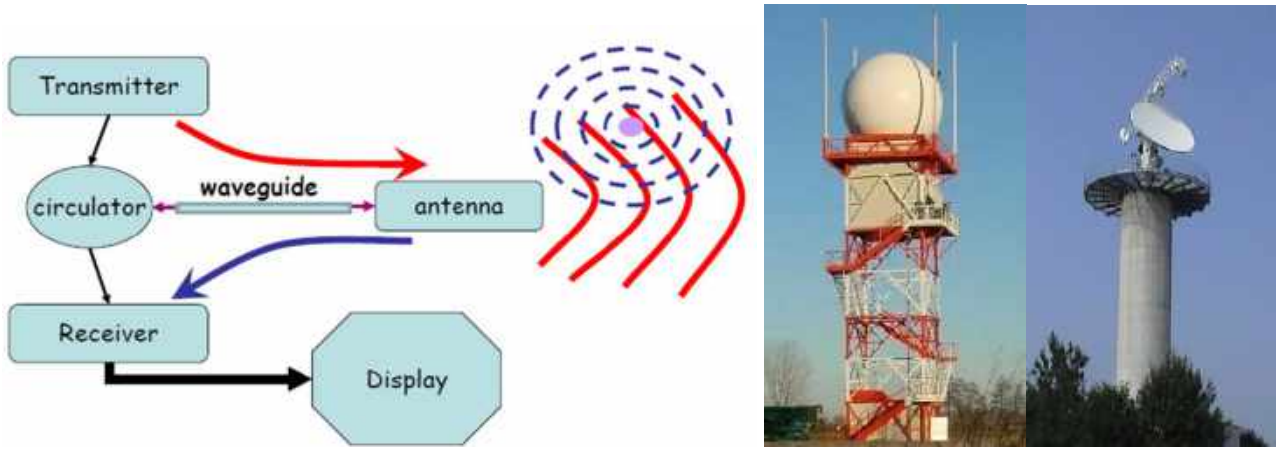

Figure 6.1.1: general radar block diagram (left) and typical radar antenna with and without radome (right)

We recall that in the framework of WP3-activity 3.2 of AdriaMORE project a weather radar composite software able to ingest and process data from systems with different features has been developed and put in operational mode utilizing Italian and Croatian radar data. This software, called CRAMS (Cetemps Radar Advanced Mosaic Software) can ingest as input both 3D raw volumes and 2D products data and gives as main output: (1) 2D products focused on extreme events for each individual radar and (2) composite radar products for weather monitoring (**figure 6.1.2**).
Detailed information about the CRAMS chain can be found in two project deliverables:
- one aimed at describing the radar's mosaic algorithm chain developed and the related composite products (**deliverable 3.2.1**);
- one aimed at describing the useful radar products to be used against extreme weather events, it can be applied at radars having different technical characteristics (**deliverable 3.2.2**).

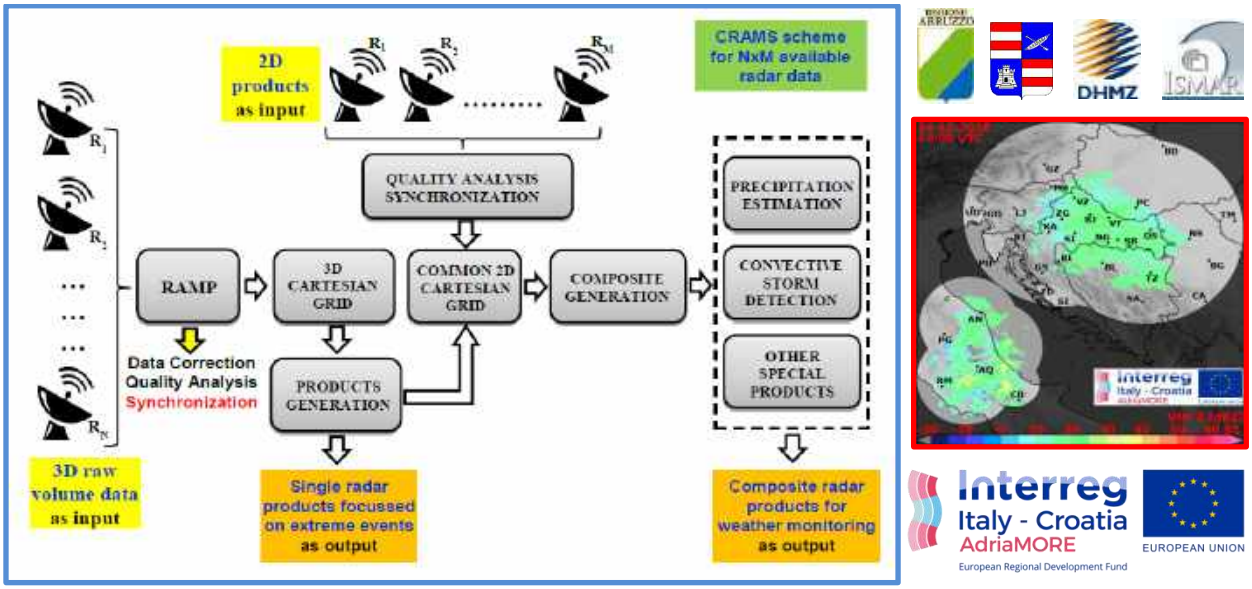

Figure 6.1.2: block diagram of the CRAMS chain developed within the AdriaMORE project

CRAMS chain has been developed in Python language (http://python.org), this is an open source, high level interpreted language with an extensive built-in standard library. It has a clear syntax, is well documented and easy to learn. Using Python also allows embedding lower-level programming languages such as C/C++ or FORTRAN. This option can be used to include external code, but also to optimise the performance of selected functions.
CRAMS has been applied on Italy and Croatian available radar (see **figure 6.1.3**) but it was built in a flexible way and can be applied to the larger domain including other radar systems.

RADAR	BAND	PEAK POWER	MAX RANGE
M. MIDIA	C	250 kW	240 Km
TORTORETO	X	25 kW	120 Km
CEPAGATTI	X	10 kW	108 Km
CINGOLI	X	25 kW	120 Km
TUFILLO	C	500 kW	175 Km
BILOGORA	S	550 kW	240 Km
PUNTIJARKA	S	550 kW	240 Km
OSIJEK	S	550 kW	240 Km

Figure 6.1.3: location and main technical features of the radars used in the CRAMS chain

For the pilot action named PAI (Pilot Action along Italian coastlines) have been used the radar installed in Italian territory. As shown in figure 6.1.3 the AdriaMORE Italian radar network is constituted by Monte Midia, Tortoreto, Cepagatti, Cingoli and Tufillo systems.

Detailed technical specifications of all radar systems are shown in **table 6.1.1** while their pictures are given in **figure 6.1.4.** In the latter figure you can also see the composite domain chosen that include most of Central Italy territories. The mosaicking domain was defined taking into account the technical characteristics of the radars, their geographical location and the peculiarities of the territory concerned. For each radar, the coverage area was set compatible with the size of the mosaicking domain, in figure 6.1.4 the coverage area utilized for each device (do not considering obstacles due to orography) is also depicted.

Features	Unit	M. Midia	Tortoreto	Cepagatti	Cingoli	Tufillo
Model	---	DWSR-93C	WR-25XP	WR-10X	WR-25XP	METEOR 660C
Data of installation	[year]	2006	2014	2016	2014	2008
Latitude	[deg]	42,06	42,78	42,40	43,36	41,94
Longitude	[deg]	13,18	13,94	14,14	13,19	14,25
Height (over sea level)	[m]	1710	10	50	790	692
Polarization capability	---	NO	YES	NO	YES	YES
Band (frequency)	[GHz]	C (5,57)	X (9,41)	X (9,41)	X (9,41)	C (5,60)
Peak Power	[kW]	250	25	10	25	500
Antenna Gain	[dB]	40,5	35	35	35	45
Range in the domain	**[km]**	**120**	**120**	**108**	**120**	**60**
Gate resolution	[m]	125	125	450	125	150
Temporal resolution	[min]	10	10	10	10	10
Beamwidth	[deg]	1,6	3,0	3,0	3,0	1,0

Table 6.1.1: technical specifications of the radars utilized on AdriaMORE Italian domain

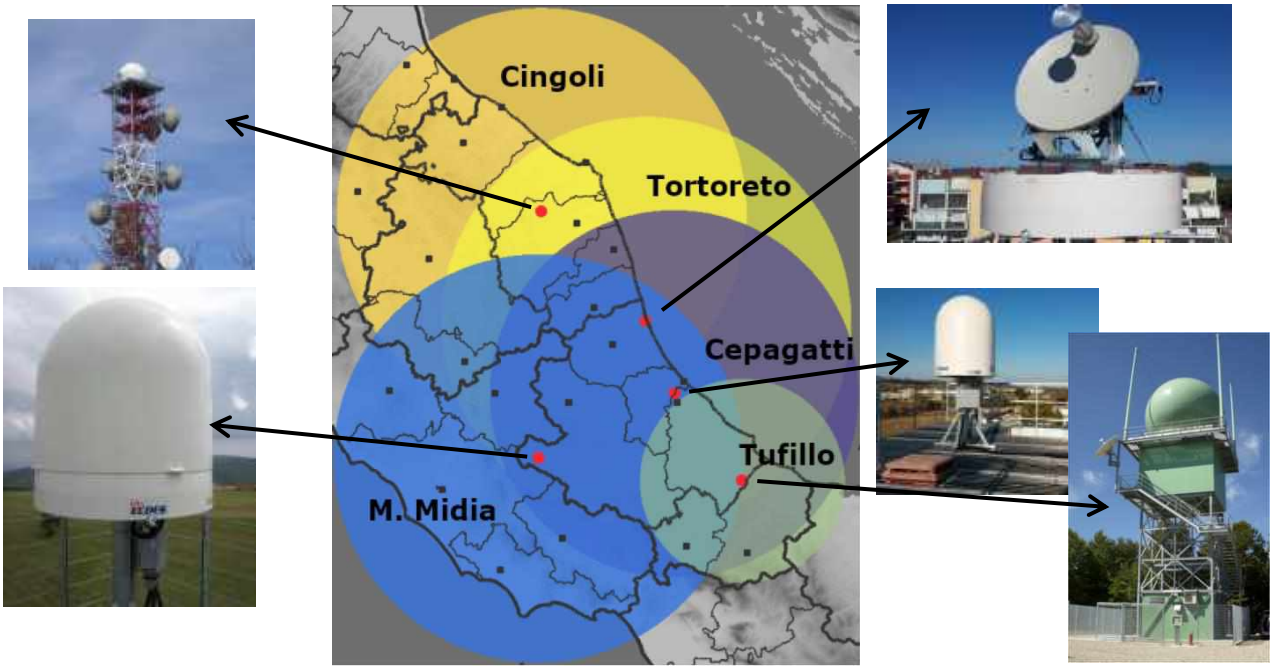

Figure 6.1.4: location and pictures of the radars utilized on AdriaMORE Italian domain

The CRAMS mosaic scheme, as applied to the Italian network, is shown in **figure 6.1.5**. In the operational configuration the implemented mosaicking software can takes as input a complete 3D volume scan from Monte Midia (MM), Cepagatti (CE) and Tortoreto (TO) radars and some 2D product from Cingoli (CI) and Tufillo (TU) radars.
All data are routinely collected every 10 minutes with synchronised start time. It is worth mentioning it is necessary to have a uniform time reference for all the radar data observations before the mosaicking. Usually the individual radars are not temporally synchronized thus a synchronization is needed both for volumetric 3D and 2D products data we have as input.

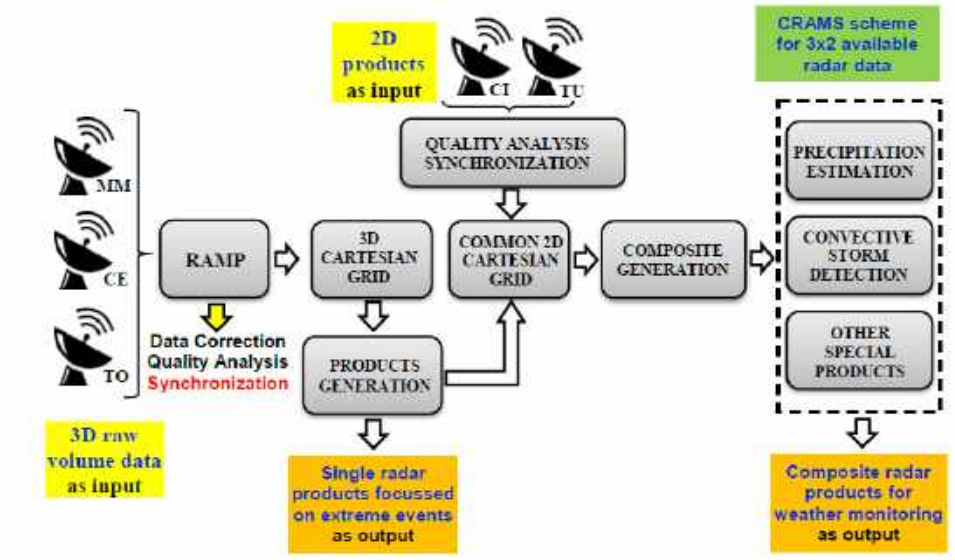

Figure 6.1.5: block diagram of the CRAMS mosaic scheme as applied to the Italian radar network

The last stage of the CRAMS chain is dedicated to the generation of composite products from the radar network for weather monitoring, they are briefly described in **table 6.1.2** while some examples of composite products are given in **figure 6.1.6**.

PRODUCT NAME	PRODUCT SYMBOL	SHORT DESCRIPTION
Vertical maximum of reflectivity	VMI	This product is useful for a quick surveillance of the composite area especially for convective precipitation to locate both mature and newly developing thunderstorm
Convective storm detection	CSD	The product is aimed at distinguish stratiform and convective areas in the composite being the latter linked to the most intense and dangerous phenomena
Surface Rainfall Intensity	SRI	This product estimates the ground instantaneous rainfall over composite area in mm/h.
Surface Rainfall Total	SRT	This product estimates the cumulated rain over composite area in mm. It can issue warnings if the precipitation in a sub catchment region exceeds a threshold value
Vertically Integrated Liquid	VIL	This product can be used as a measure for the potential strong rainfall
Hail detection	POH	The product is aimed at hail detection which is one of the most danger phenomena

Table 6.1.2: brief description of the composite products implemented within CRAMS chain

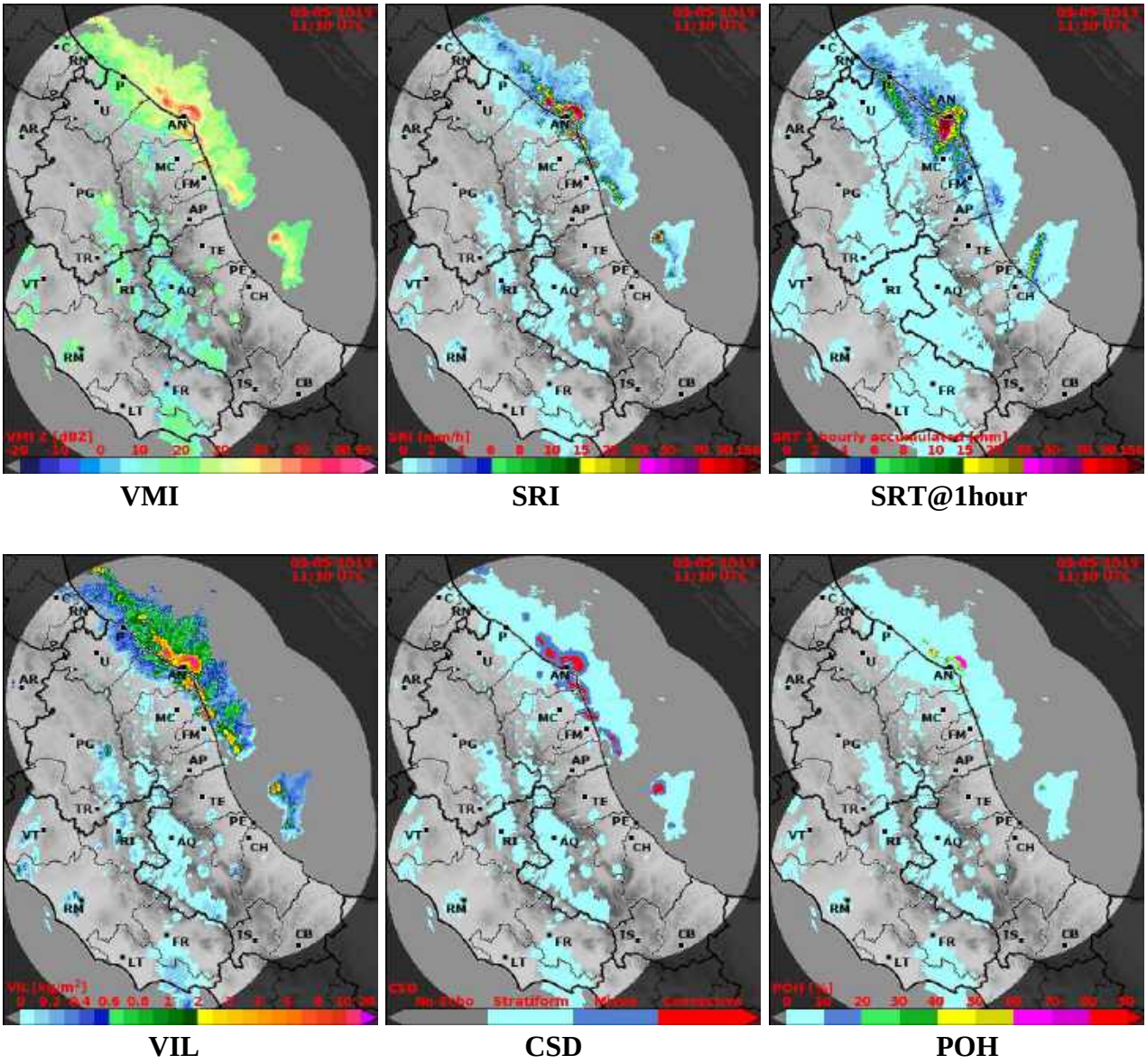

Figure 6.1.6: example of composite products for the Italian network

A work entitled "Inter-regional mosaic of X-band radar data for observation of extreme events in the Adriatic area" was presented to the third national Radar meteorology conference (RadMet 2019) was held in Turin from 3 to 4 July 2019. As in the two previous editions, the conference aims to stimulate dialogue and exchange of experiences between the realities that in Italy develop and use, both in the operational and research fields, weather radar for observing and forecasting precipitation events. The work focuses on the description of X-band systems in Abruzzo and Marche, on the data processing chain and on the mosaic process. The hydrological risks of these two regions are further enhanced by their complex orography, in these conditions, the monitoring of precipitation with high-space-time resolution radar can allow to significantly increase the statistics of extreme events identified. The contribution of the Italy-Croatia Cross-Border Cooperation Program (2014-2020) through the AdriaMORE project was well highlighted.

A WEB interface has been arranged at *http://radar.aquila.infn.it/network/*, where the instantaneous rainfall estimates for the Croatian and Italian composites are displayed in real-time.
The radar data flow towards CETEMPS has been implemented operationally with the development of an automatic procedure that allows to receive the available data (volumes or products) in real time to be displayed. Furthermore, only for the Italian composite, is shown a loop with the last reflectivity images (VMI product) useful to follow the evolution of the phenomenon in progress (**figure 6.1.7**). The Italian maps are updated every 10 minutes, the Croatian ones every 15 minutes following the scanning frequencies set by the individual administrations involved.

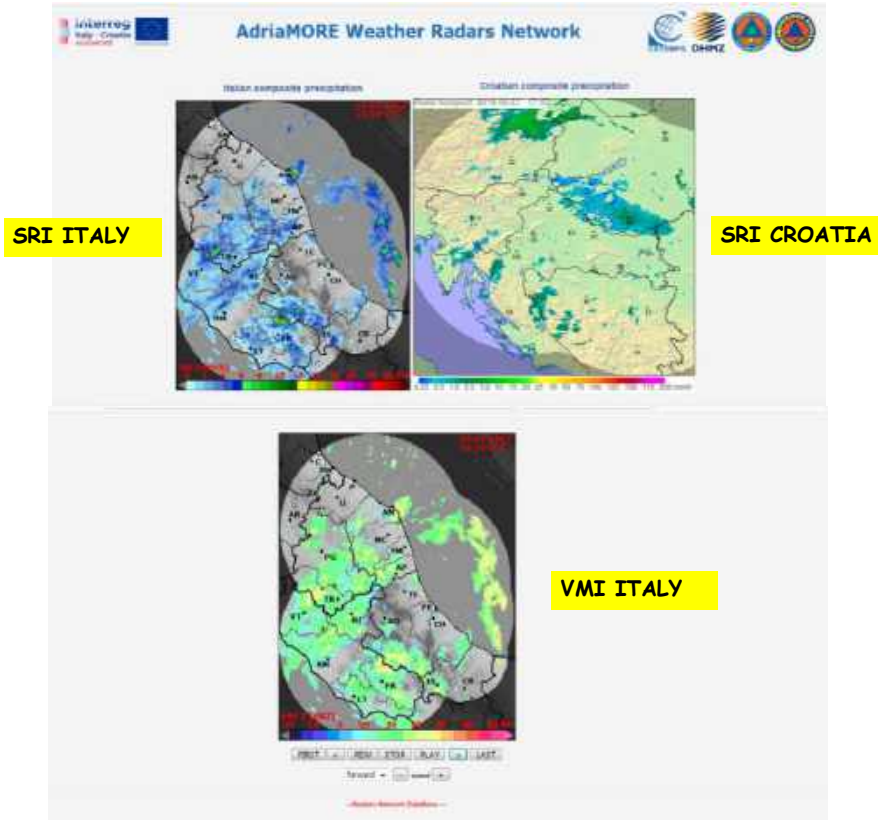

Figure 6.1.7: web interface developed under AdriaMORE project with SRI and VMI products displayed in real time, it is available at http://radar.aquila.infn.it/network/ and in MyDewetra DSS

The case study occurred in central Italy territory along Adriatic area on May 12-14, 2019 have been analyzed by using the Italian composite thanks the large availability of the data. In **figure 6.1.8-6.1.10** the time evolution of the precipitation is shown by using VMI composite products while in **figure 6.1.11** an example of accumulated precipitation (SRT) on various hours is depicted. In figures **6.1.12** and **6.1.13** some other composite products (SRI, CSD, VIL and POH) are shown for May 13 and 14 respectively at certain instants. The maps on May 13 are in-line with the mixed characteristic of the precipitation that is medium values of SRI and VIL as well as the presence of few convective areas in the CSD and low POH values (no hail event has occurred) while the maps on May 14 are in-line with the stratiform characteristic of the precipitation that is low values of SRI and VIL as well as absences of convective areas in the CSD and null POH values. In such days the composite product maps have similar behavior in other hours too.

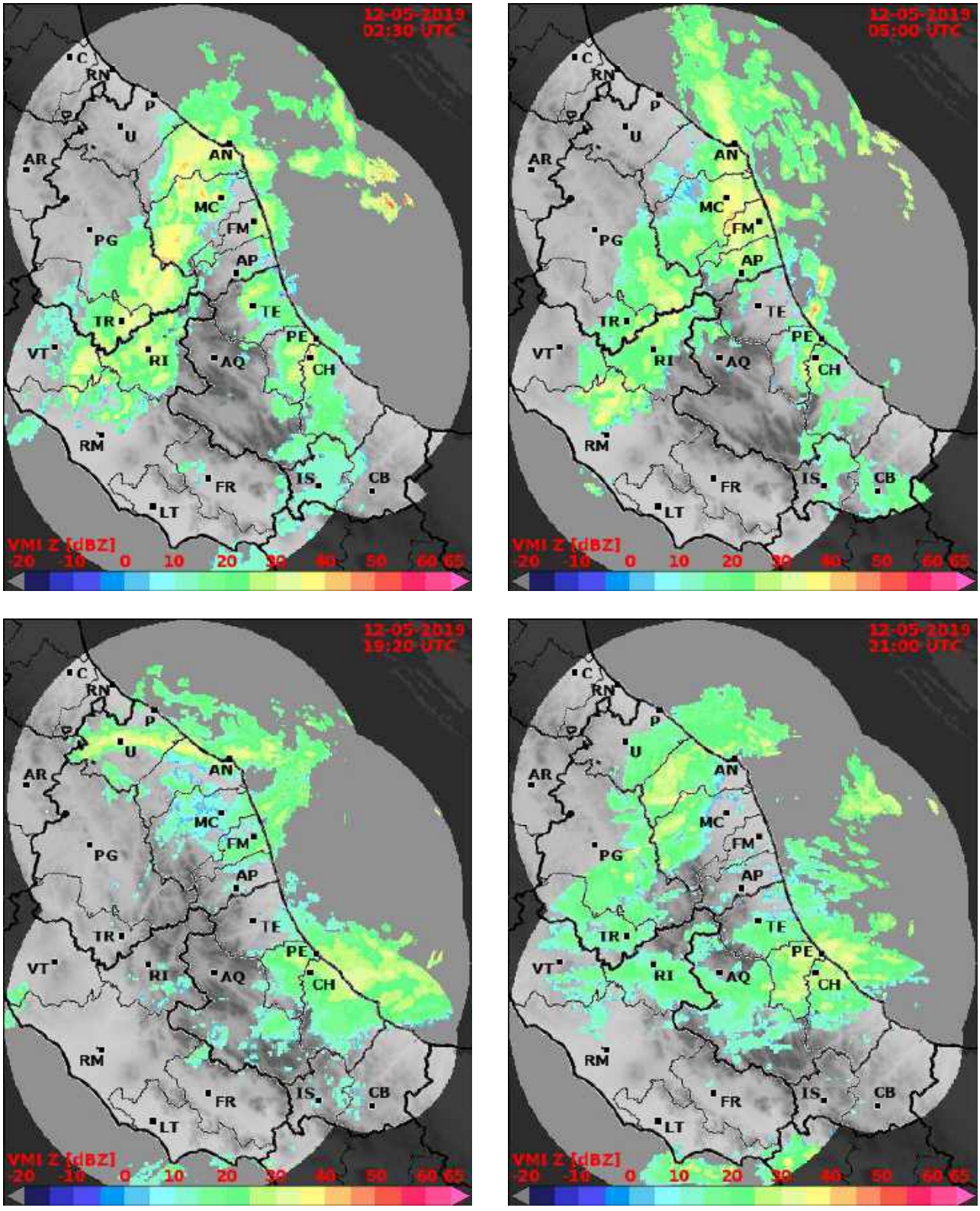

Figure 6.1.8: some images of AdriaMORE radar network for VMI product taken on May 12, 2019

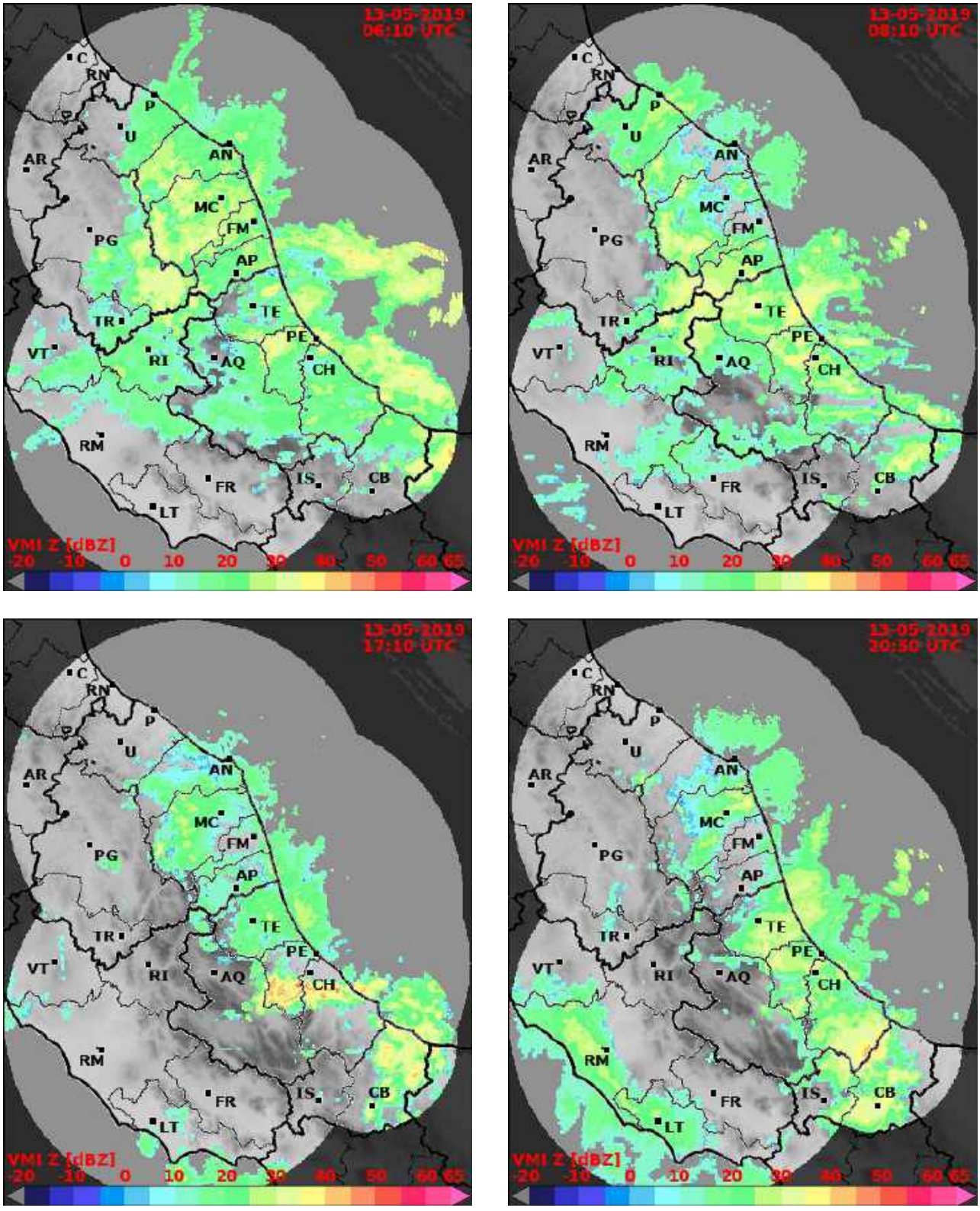

Figure 6.1.9: some images of AdriaMORE radar network for VMI product taken on May 13, 2019

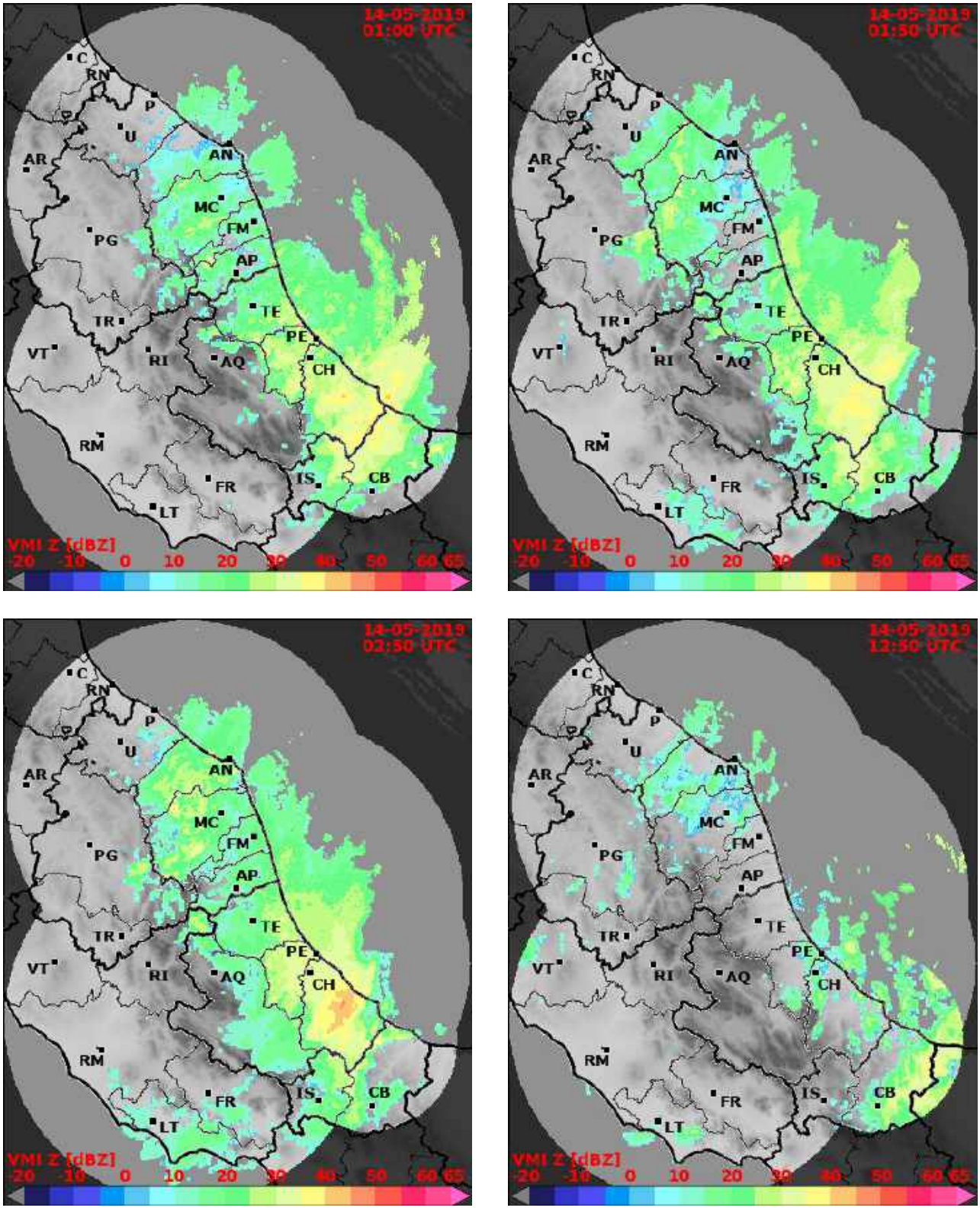

Figure 6.1.10: some images of AdriaMORE radar network for VMI product taken on May 14, 2019

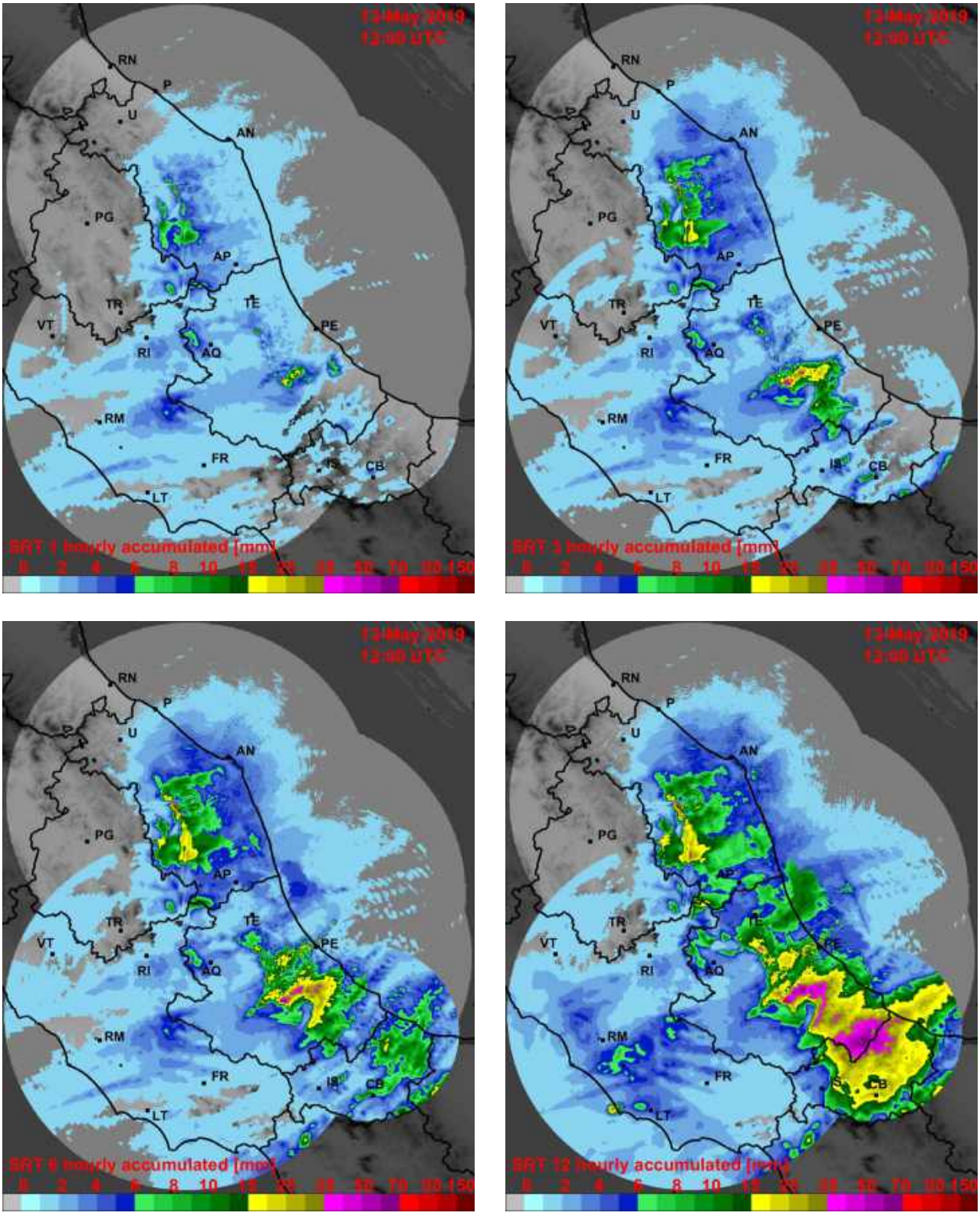

Figure 6.1.11: images of composite AdriaMORE radar network for SRT product on May 13, 2019 starting from 12:00 UTC with 1-hour accumulated (top left), 3-hour accumulated (top right), 6-hour accumulated (bottom left) and 12-hour accumulated (bottom right)

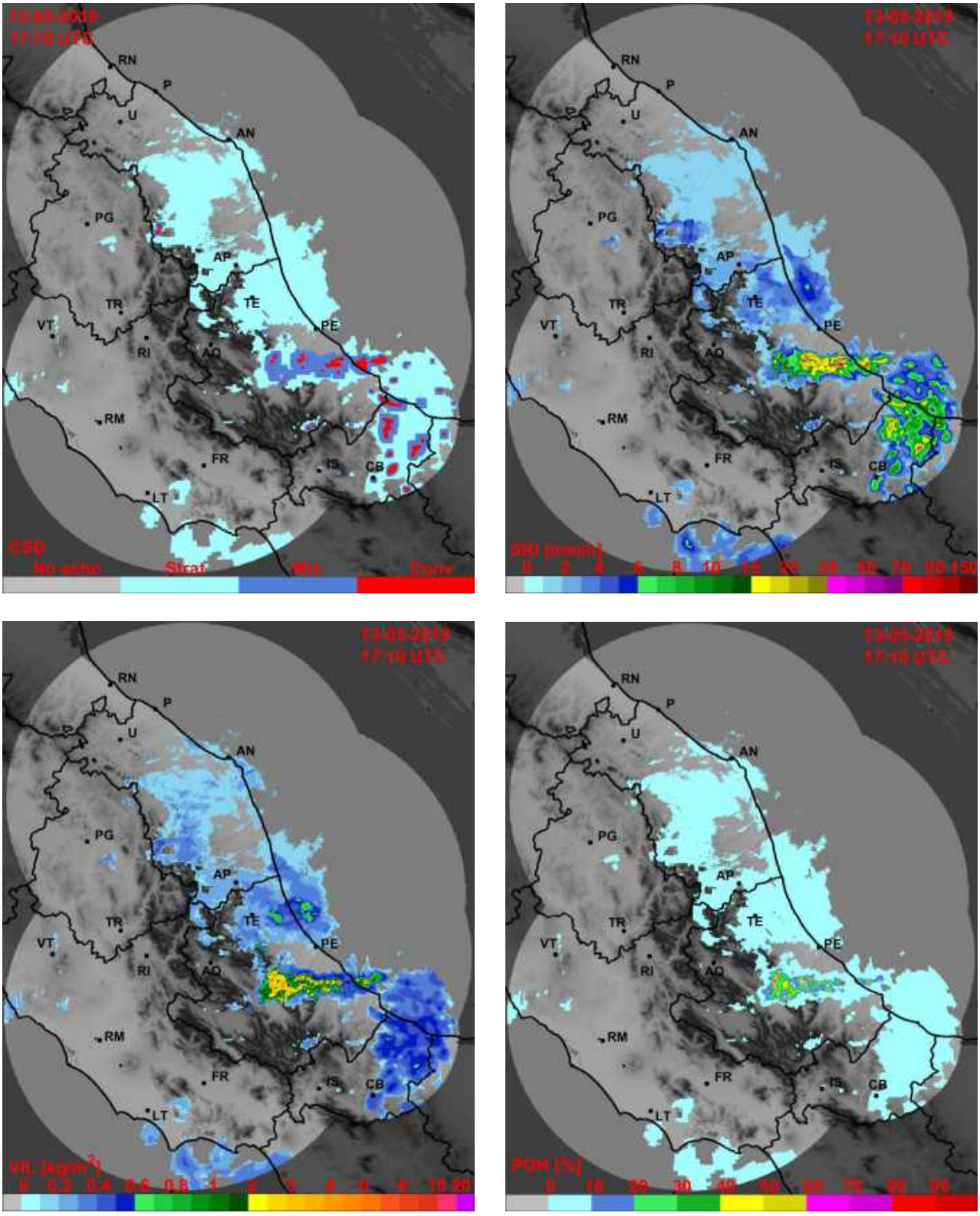

Figure 6.1.12: images of composite AdriaMORE radar network products on May 13, 2019 at 17:10 UTC, are shown CSD (top left) SRI (top right), VIL (bottom left) and POH (bottom right)

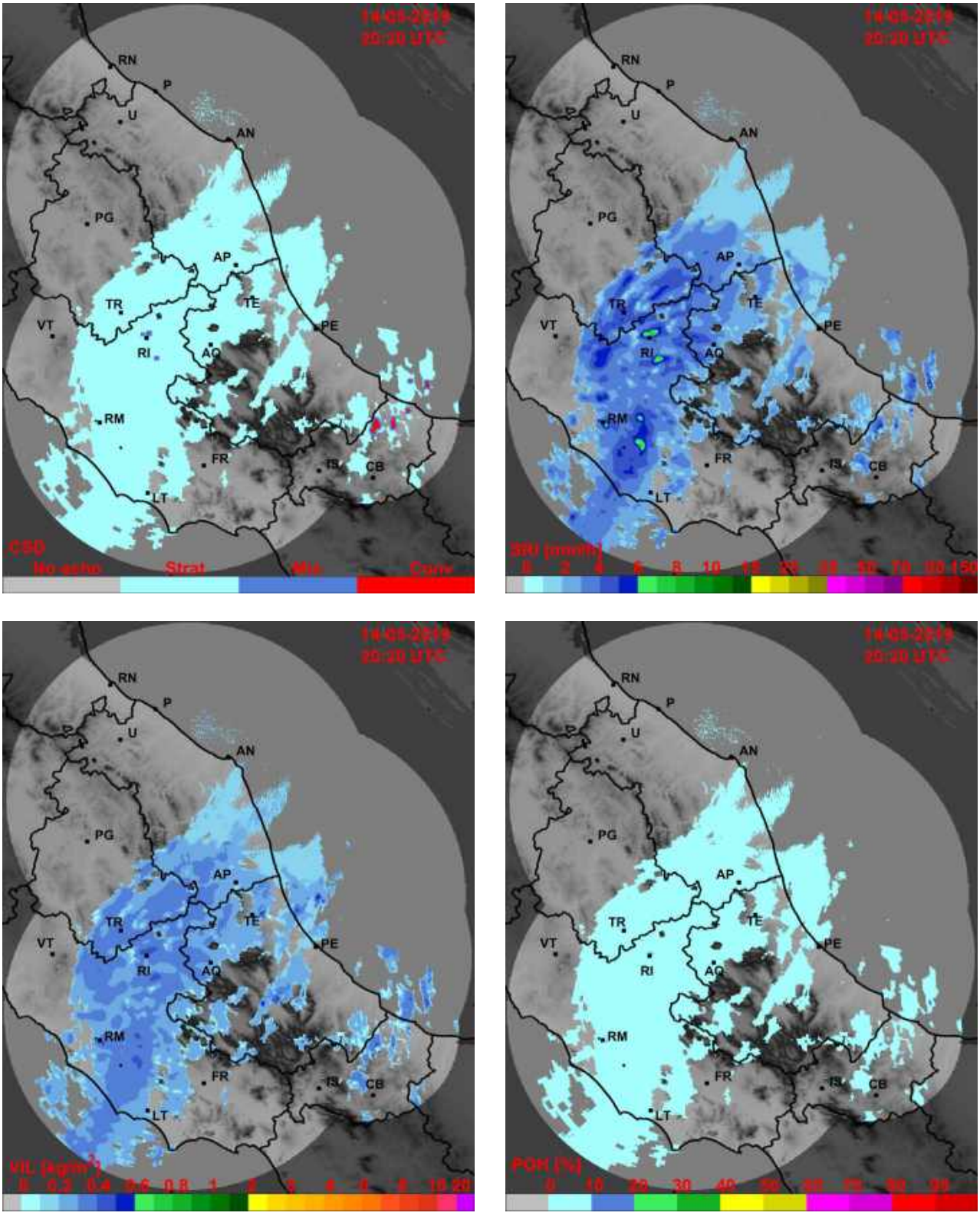

Figure 6.1.13: images of composite AdriaMORE radar network products on May 14, 2019 at 20:20 UTC, are shown CSD (top left) SRI (top right), VIL (bottom left) and POH (bottom right)

6.2 Rain gauges network

Acquisition and processing of rainfall data from rain gauges are performed by Italian regional authorities at different time intervals, ranging from 5 to 30 min.

The data of the rain gauge network are collected through the telephone networks for communication (fixed-line or low-power cellular network) and the UHF/VHF radio link to be processed, centrally in near real time, by the Italian Department of Civil Protection (DPC). The latter distributes products related to instantaneous precipitation and accumulated to the hydrological and meteorological regional services.

Quality control of these rain gauges measurement data is the first step in the context of an operational use of the data.

Therefore, the rainfall data has been preliminarily subjected to a quality control in order to identify and remove any inconsistencies. The quality control carried out includes the following actions:

1) control of rain gauges with the same name but different coordinates;
2) removal of data associated with rain gauges without valid coordinates;
3) removal of duplicate data;
4) control of the same rain gauges with different values at the same time;
5) control of rain gauges with an instantaneous precipitation rate too high;
6) identification of anomalous data (for example very different values respect to the surrounding rain gauges).

Gauge data can be spatially interpolated and can be displayed in various ways, find in the following a brief analysis on the case study on May 12-14, 2019 by using MyDewetra platform visualization.

In **figures 6.2.1** the accumulated rain map, on center Italy, for the whole event is shown, the major rainfall (around 120-150 mm) are localized along the Apennines ridge and in Adriatic coastal area including Marche and Abruzzi regions (60-90 mm). The daily accumulated rainfall on May 12, 13 and 14, are shown in **figures 6.2.2-6.2.4,** they point out the rainy movement along Adriatic area, moreover reveal as the maximum precipitation occurred on May 13, 2019. The same evolution, through six hours accumulated rainfall, are shown in **figures 6.2.5-6.2.13**.

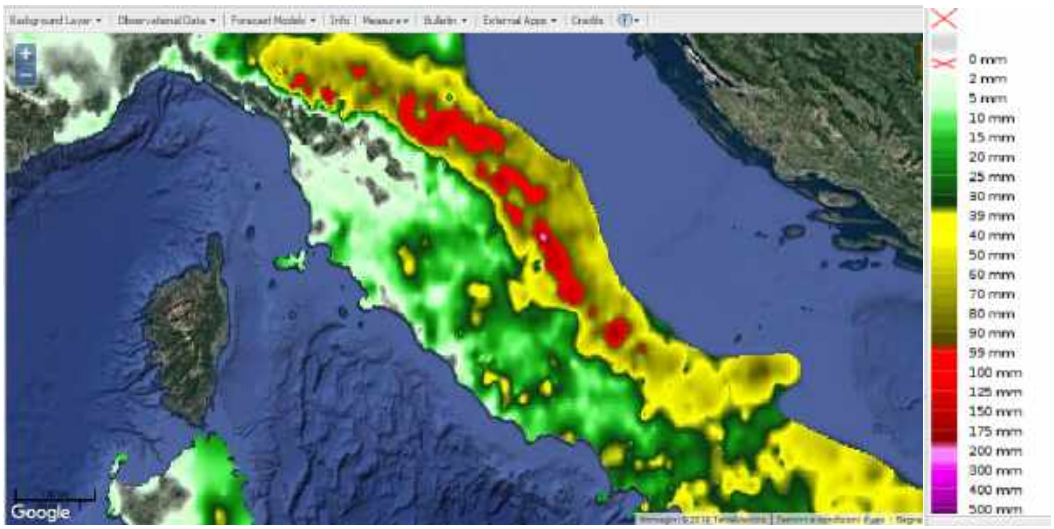

Figure 6.2.1: three days accumulated rainfall from May 12 to May 14, 2019

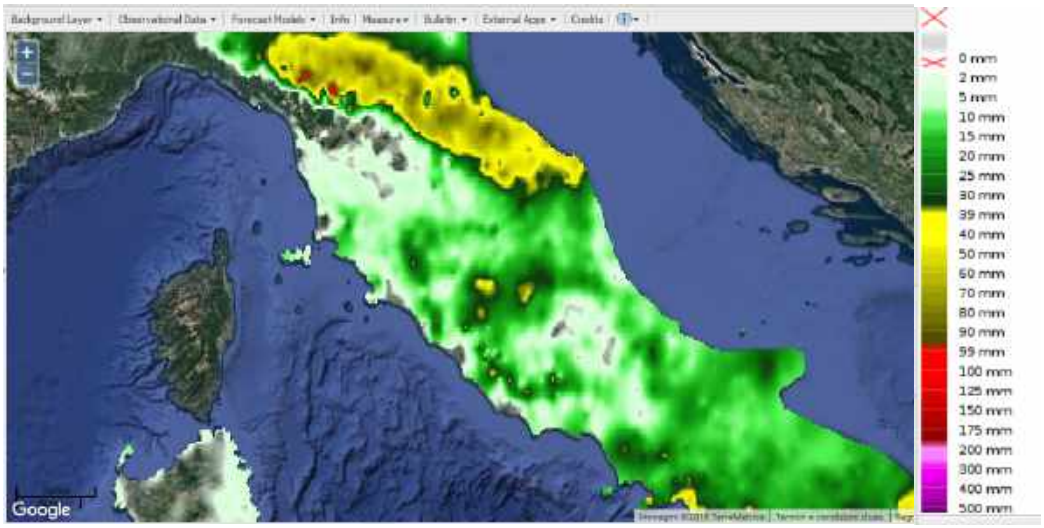

Figure 6.2.2: daily accumulated rainfall on May 12, 2019

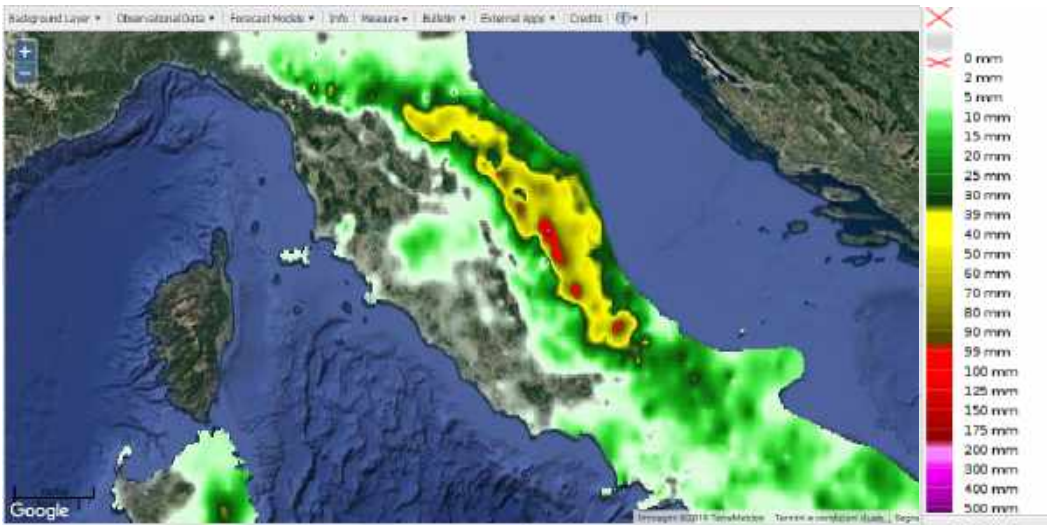

Figure 6.2.3: daily accumulated rainfall on May 13, 2019

Figure 6.2.4: daily accumulated rainfall on May 14, 2019

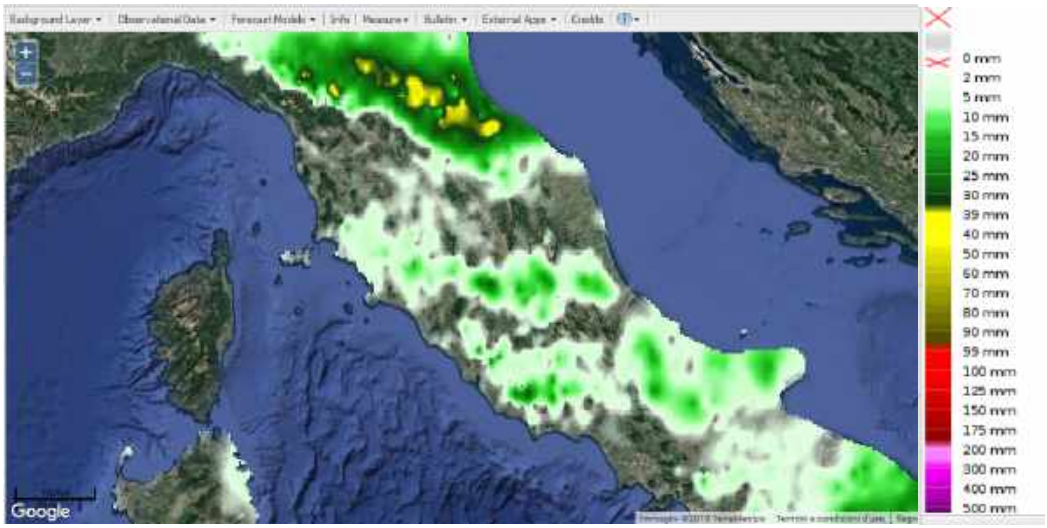

Figure 6.2.5: six hours accumulated rainfall on May 12, 2019 from 12:00 to 18:00 UTC

Figure 6.2.6: six hours accumulated rainfall on May 12, 2019 from 18:00 to 24:00 UTC

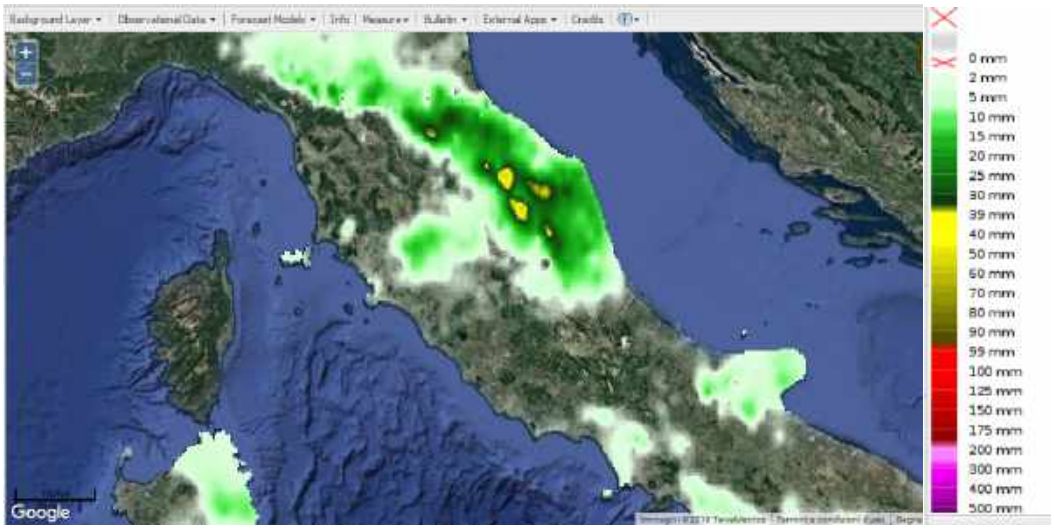

Figure 6.2.7: six hours accumulated rainfall on May 13, 2019 from 00:00 to 06:00 UTC

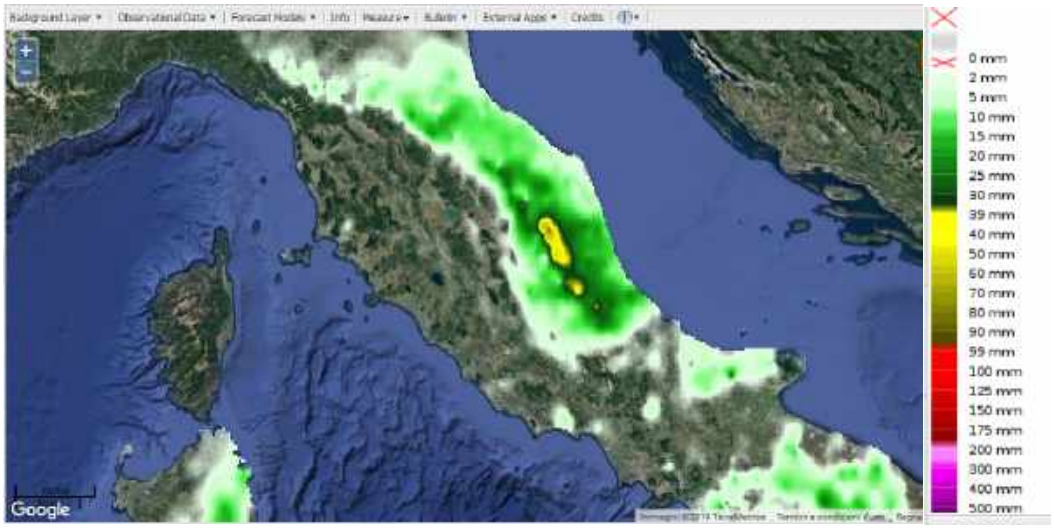

Figure 6.2.8: six hours accumulated rainfall on May 13, 2019 from 00:06 to 12:00 UTC

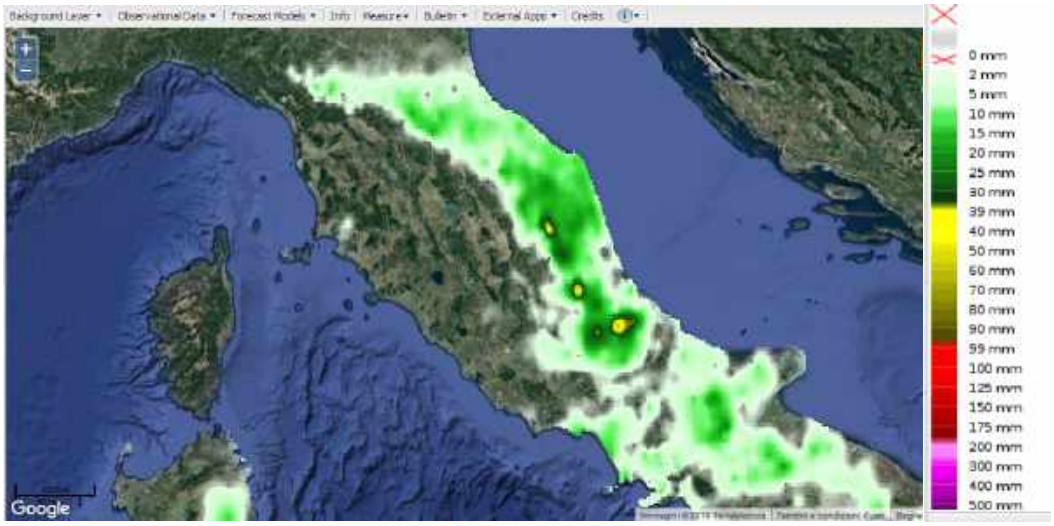

Figure 6.2.9: six hours accumulated rainfall on May 13, 2019 from 12:00 to 18:00 UTC

Figure 6.2.10: six hours accumulated rainfall on May 13, 2019 from 18:00 to 24:00 UTC

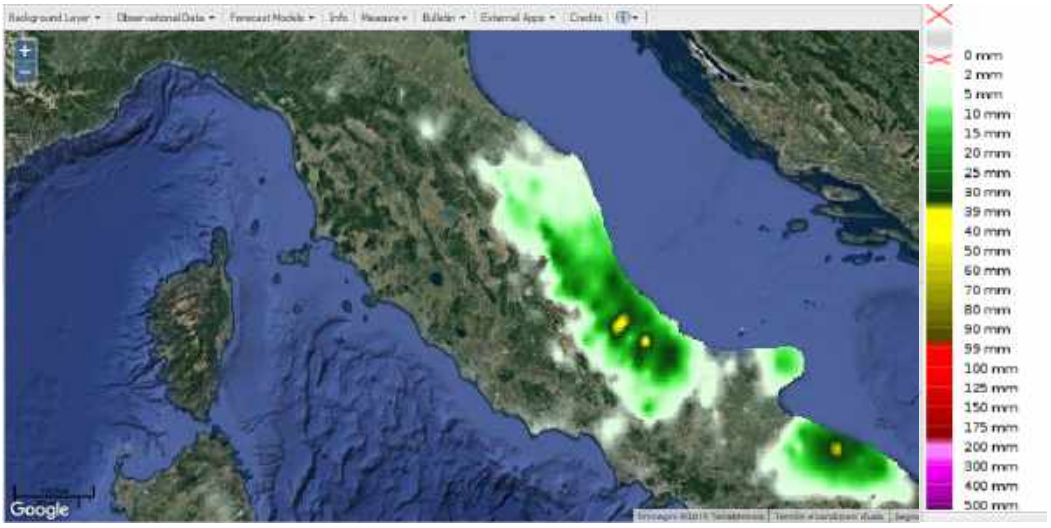

Figure 6.2.11: six hours accumulated rainfall on May 14, 2019 from 00:00 to 06:00 UTC

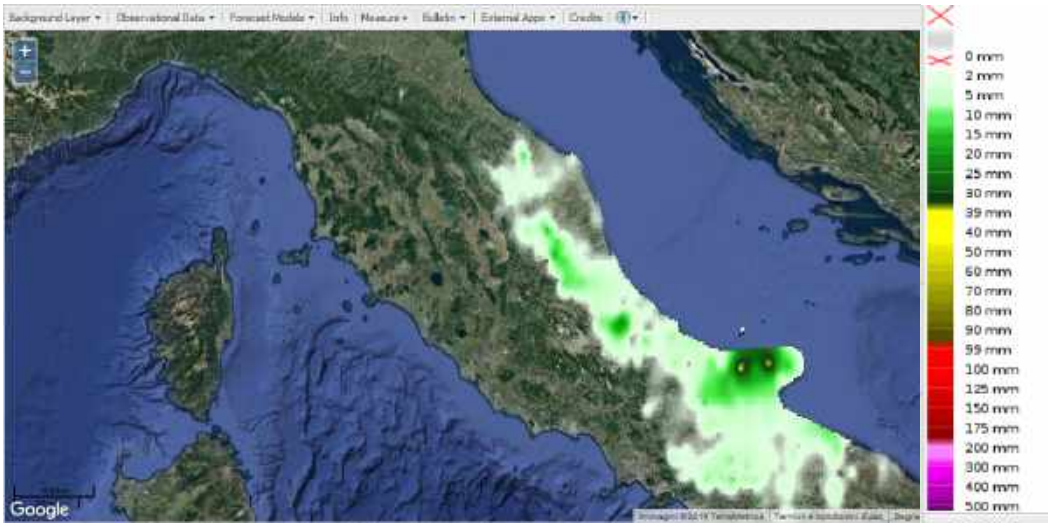

Figure 6.2.12: six hours accumulated rainfall on May 14, 2019 from 06:00 to 12:00 UTC

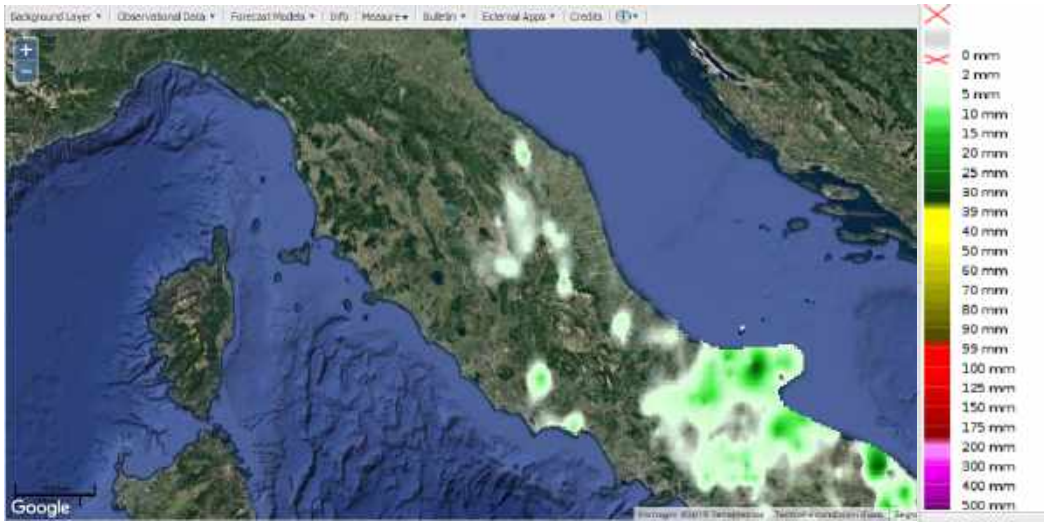

Figure 6.2.13: six hours accumulated rainfall on May 14, 2019 from 12:00 to 18:00 UTC

6.3 Satellite rain retrieval

A procedure for extracting surface rain estimation from satellite-based observations was developed in the framework of ADRIARadNet project. In particular, surface rain is estimated from infrared radiometric observations or brightness temperature (BT), collected by Meteosat Second Generation (MSG) geostationary satellite, and calibrated by using ground-based available weather radar data. The general idea behind the procedure is to combine the appealing coverage and spatial/temporal resolution of geostationary BT observations with more accurate rain rate estimates from radars which suffer of a limited spatial/temporal resolution and coverage.

The AdriaMORE Italian weather radar network has been chosen to be the source of surface rain intensity (SRI in mm/h), with its high accuracy and resolution. Thus, the correlation between satellite-based BT observations and radar-derived SRI is used to extend the SRI product from the AdriaMORE weather radar network to the whole Adriatic basin.

The statistical integration technique is built within a procedure that runs continuously over the Adriatic domain. This procedure, called MICRAdria (Microwave Infrared Combined Rainfall Algorithm for Adriatic regions), is based on a background process and a foreground process.

During the background process, the latest nearly-simultaneous SRI products from the weather radar network and BT observations are spatially collocated. The set of SRI-BT matchups is then used to calibrate a SRI-BT relationship through a statistical integration technique.

During the foreground process, the latest coefficients are applied to estimate the rain rate from the next BT observations over the entire Adriatic domain. The process is iterated every time step (30 minutes) and it is continuously ongoing, since new SRI and BT data are continuously ingested.

An example of output is shown in the **figure 6.3.1** where the SRI product (in mm/h) is color-coded according to the horizontal bar. The real time image is available at the web link http://radar.aquila.infn.it/micra/ as well as in MyDewetra platform.

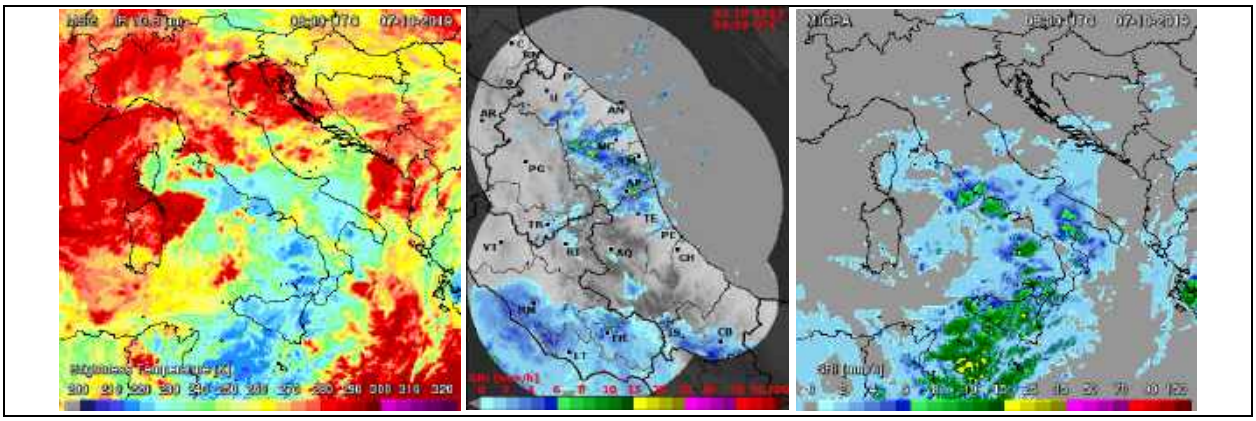

Figure 6.3.1: MICRAdria application on October 7, 2019 at 08:00 UTC, in the left panel BT measured by MSG channel 9, in the central panel the SRI product from the AdriaMORE Italian radar network and in the right panel the SRI derived from MICRAdria procedure

For the case study occurred in central Italy territory along Adriatic area on May 12-14, 2019 in **figures 6.3.2-6.3.4** are shown some SRI maps derived from MICRAdria procedure taken from MyDewetra platform.

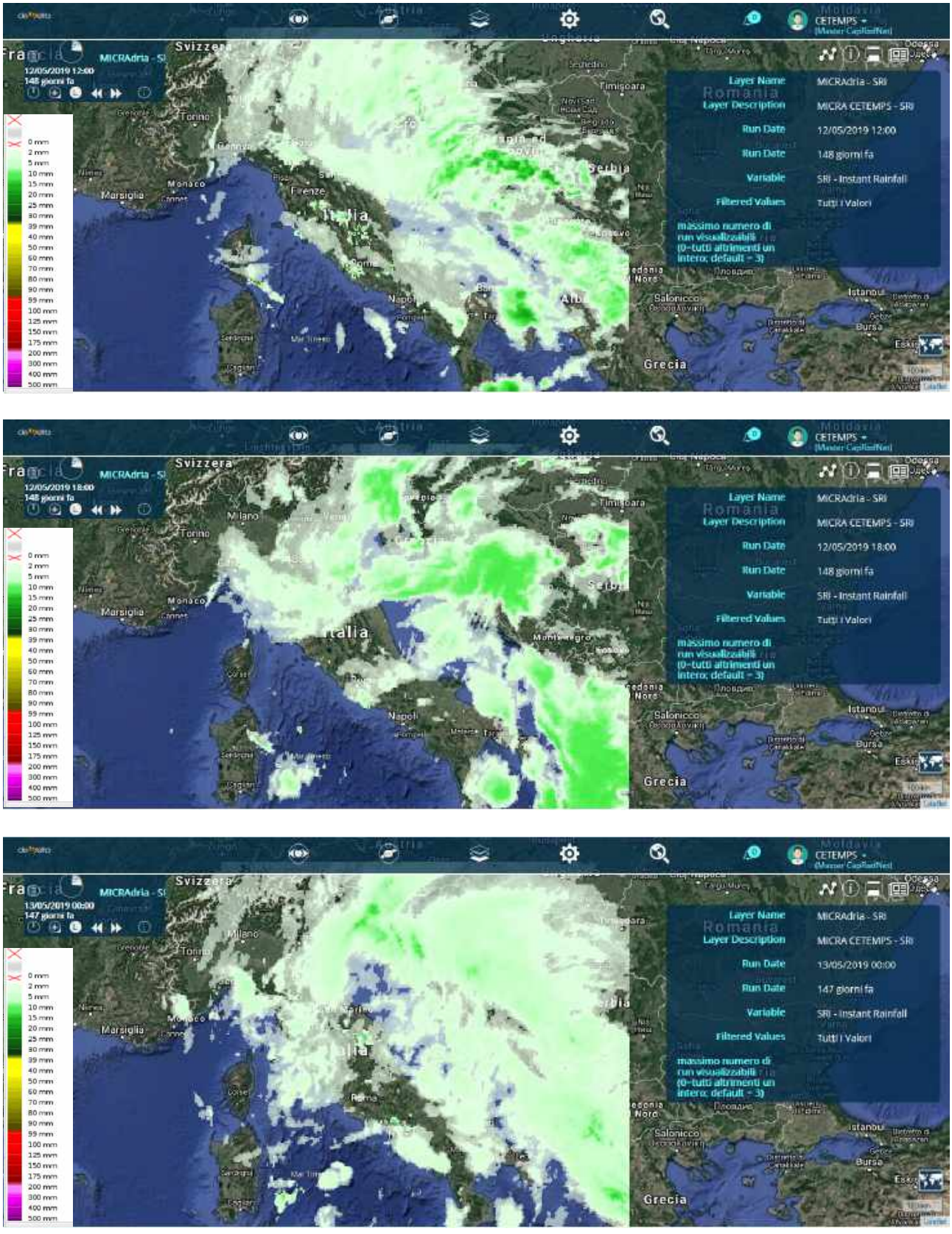

Figure 6.3.2: MICRAdria SRI maps taken from MyDewetra platform on May 12, 2019 at 12:00 UTC (top panel) ,18:00 (central panel) and 24:00 UTC (bottom panel)

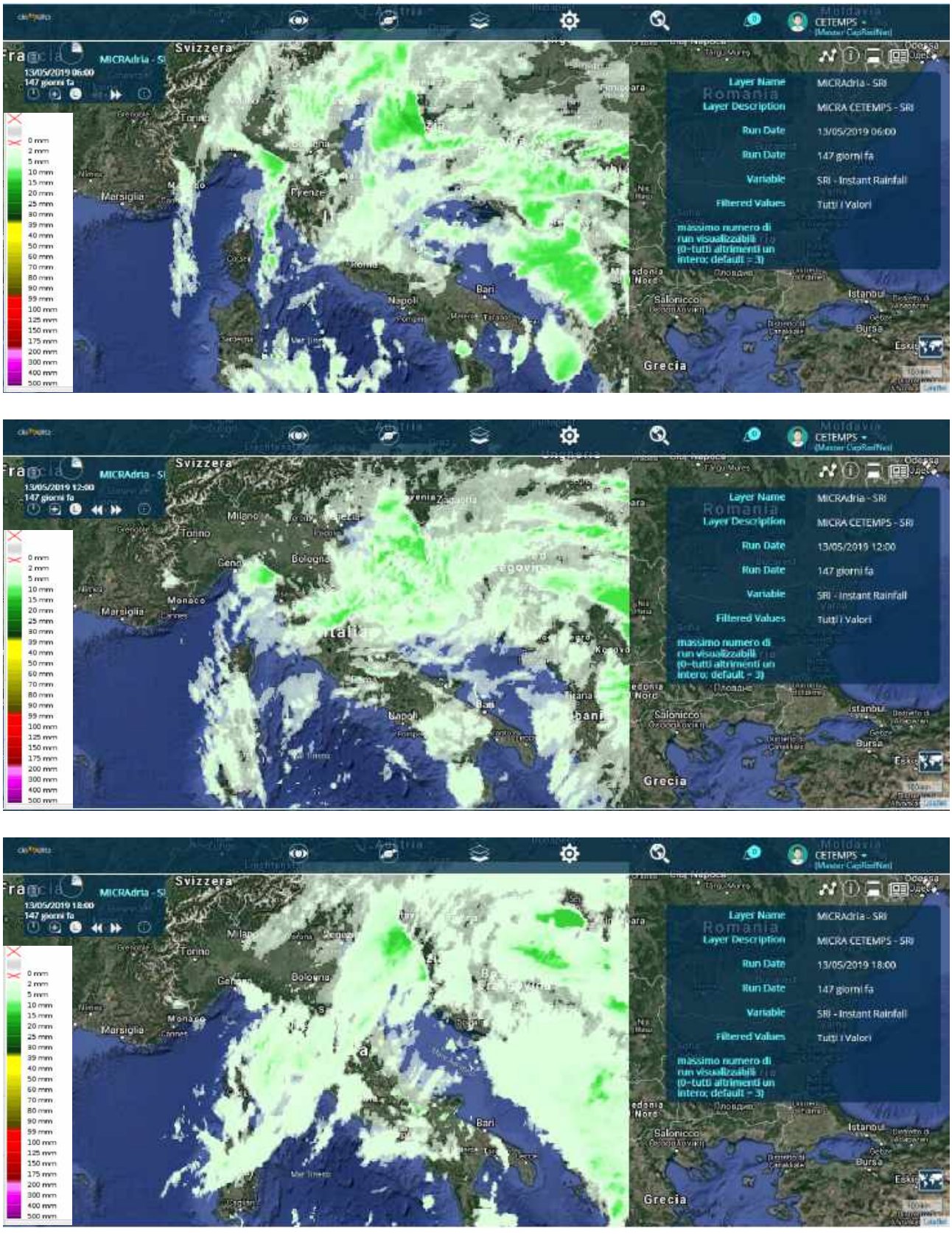

Figure 6.3.3: MICRAdria SRI maps taken from MyDewetra platform on May 13, 2019 at 06:00 UTC (top panel) ,12:00 (central panel) and 18:00 UTC (bottom panel)

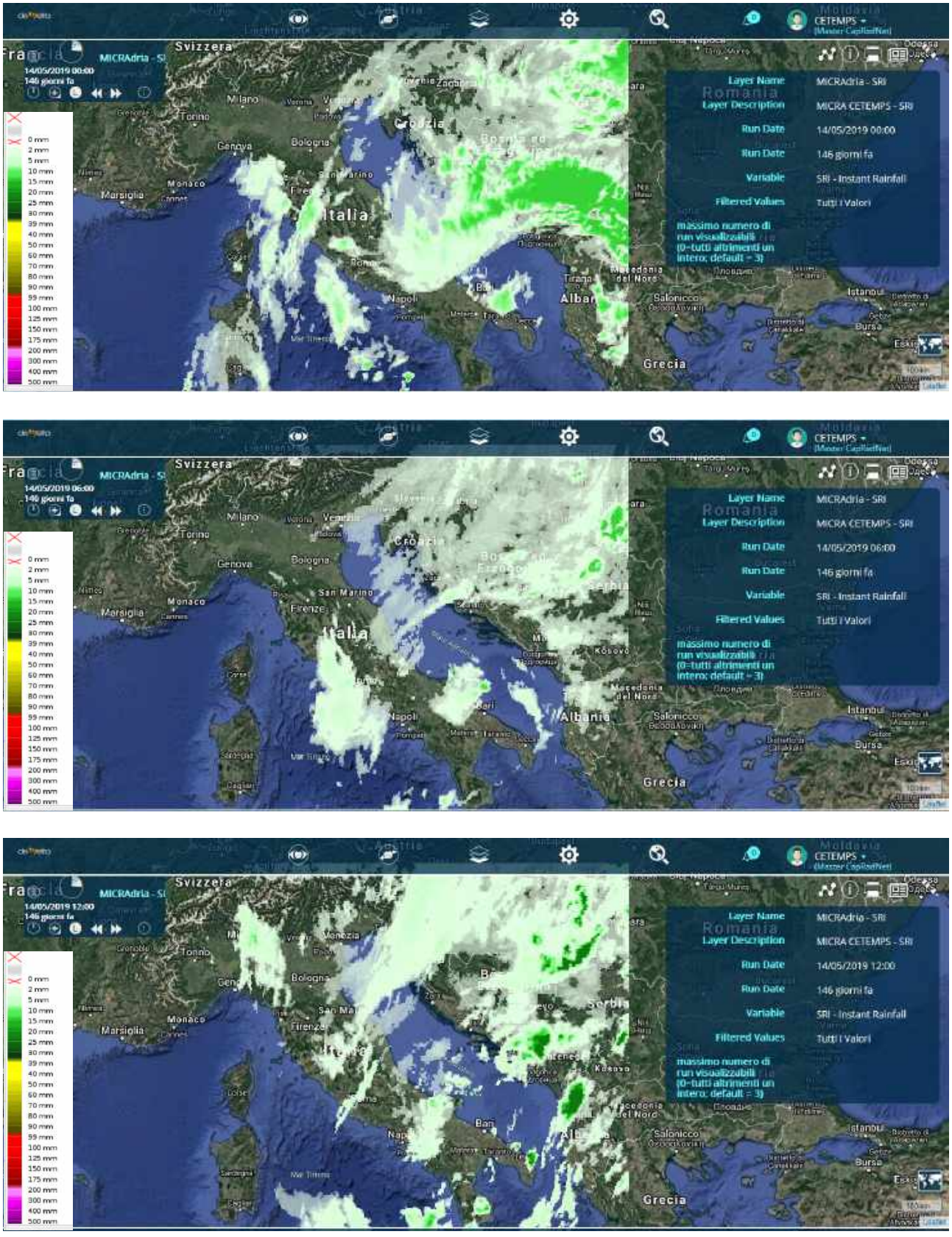

Figure 6.3.4: MICRAdria SRI maps taken from MyDewetra platform on May 14, 2019 at 00:00 UTC (top panel) ,06:00 (central panel) and 12:00 UTC (bottom panel)

6.4 Lightning network

A lightning discharge emits radio frequency energy over a wide range of frequencies. When high currents occur in previously ionized channels during cloud-to-ground flashes, the most powerful emissions occur in the very low frequency (VLF) range, the latter refers to radiofrequencies in the range of 3 kHz to 30 kHz. An essential advantage of low frequencies in contrast to higher frequencies is the property that these signals are propagated over thousands of kilometers by reflections from the ionosphere and the ground. In general, a lightning discharge generates several short duration pulses running between a storm cloud and the ground, or between or within storm clouds.

Two ground-based networks of lightning sensors have been used for AdriaMORE pilot action purpose: they are the LAMPINET and the BLITZORTUNG network, depending on their availability.

The LAMPINET network data is available on MyDewetra platform, offering the localization and the intensity of the lightning strikes observed through the SFLOC method (acronym for 'Sferic location'). A 'spherical' interference is caused by radio waves emitted by a lightning or a thunder. From the measurement of the time-of-arrival of the interference it can be inferred, through suitable sensors, the location of the phenomenon. The LAMPINET network became operational in 2004 and currently consists of 15 sensors distributed on the whole Italian territory. In its current configuration, LAMPINET measures with an accuracy of detection higher than 90% for amperage higher than 5 kA and a 500-meter localization precision.

BLITZORTUNG is a voluntary network employing VLF lightning receivers sites and one central processing server for each larger region. The receiver sites transmit their data in short time intervals over the Internet to central server. Every data sentence contains the precise time-of-arrival of the received lightning strike impulse and the geographic position of the receiver site. With this information from all receiver sites the exact positions of the discharges are computed. Lightning data are released every minute with expected accuracy of lightning localization of about some kilometers in the central Italy. BLITZORTUNG data are available on CETEMPS website.

An example of output, from the two different network, is shown in the figures below.

<table>
<tr>
<td> 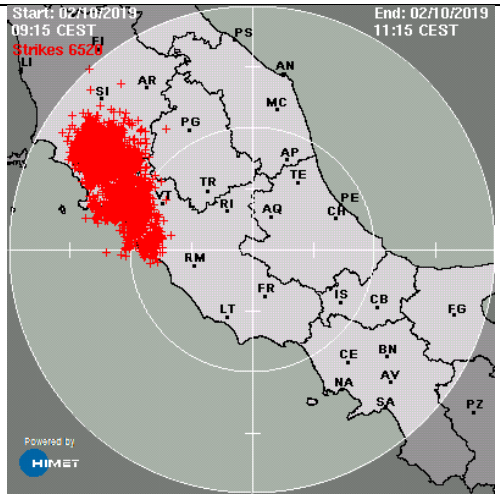
</td>
<td> 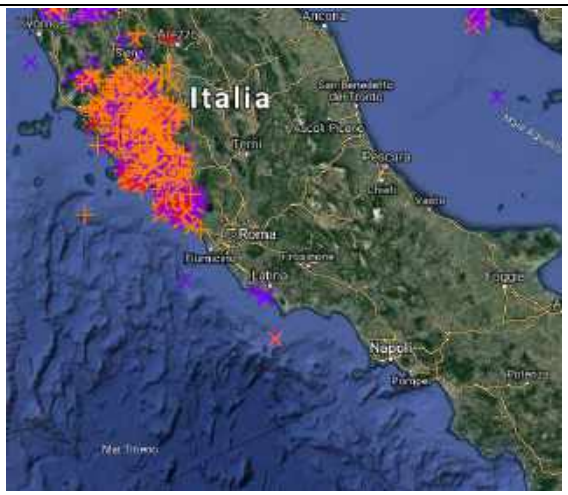
</td>
</tr>
<tr>
<td>Number and locations of lightning taken from BLITZORTUNG network on 2 October 2019 from 07:15 to 09:15 UTC</td>
<td>Locations of lightning taken from LAMPINET network on 2 October 2019 from 06:15 to 09:15 UTC</td>
</tr>
</table>

In MyDewetra, the lightning derived from LAMPINET network can be visualized with 5, 15, 30, 60 minutes and 3, 6, 24 hour time range.
For the case study occurred in central Italy along Adriatic area on May 12-14, 2019 some examples of lightning maps derived from MyDewetra platform are shown.
In **figure 6.4.1** you can see the localization and the intensity (expressed as positive or negative amperage) of the lightning strikes observed on May 12 in the past three hours starting from 05:00 UTC. **In figure 6.4.2** is shown the same map of figure 6.4.1 but with an accumulated period of six hours, to note the high number of strikes along the Adriatic sea.
In figure 6.4.3 are shown the localization and the intensity of the lightning strikes observed during the whole days of 12, 13 and 14 May 2019, to note the absence of lightning strikes in the Pescara area for the entire focused period, therefore there were no significant convective storm. That in agreement with POH and CSD maps carried out from the Italian composite.

Figure 6.4.1: location and the intensity (expressed as positive or negative amperage) of the lightning strikes observed on May 12, 2019 from 02:00 to 05:00 UTC

Figure 6.4.2: location and the intensity (expressed as positive or negative amperage) of the lightning strikes observed from May 11, 2019 at 23:00 UTC to May 12, 2019 at 05:00 UTC

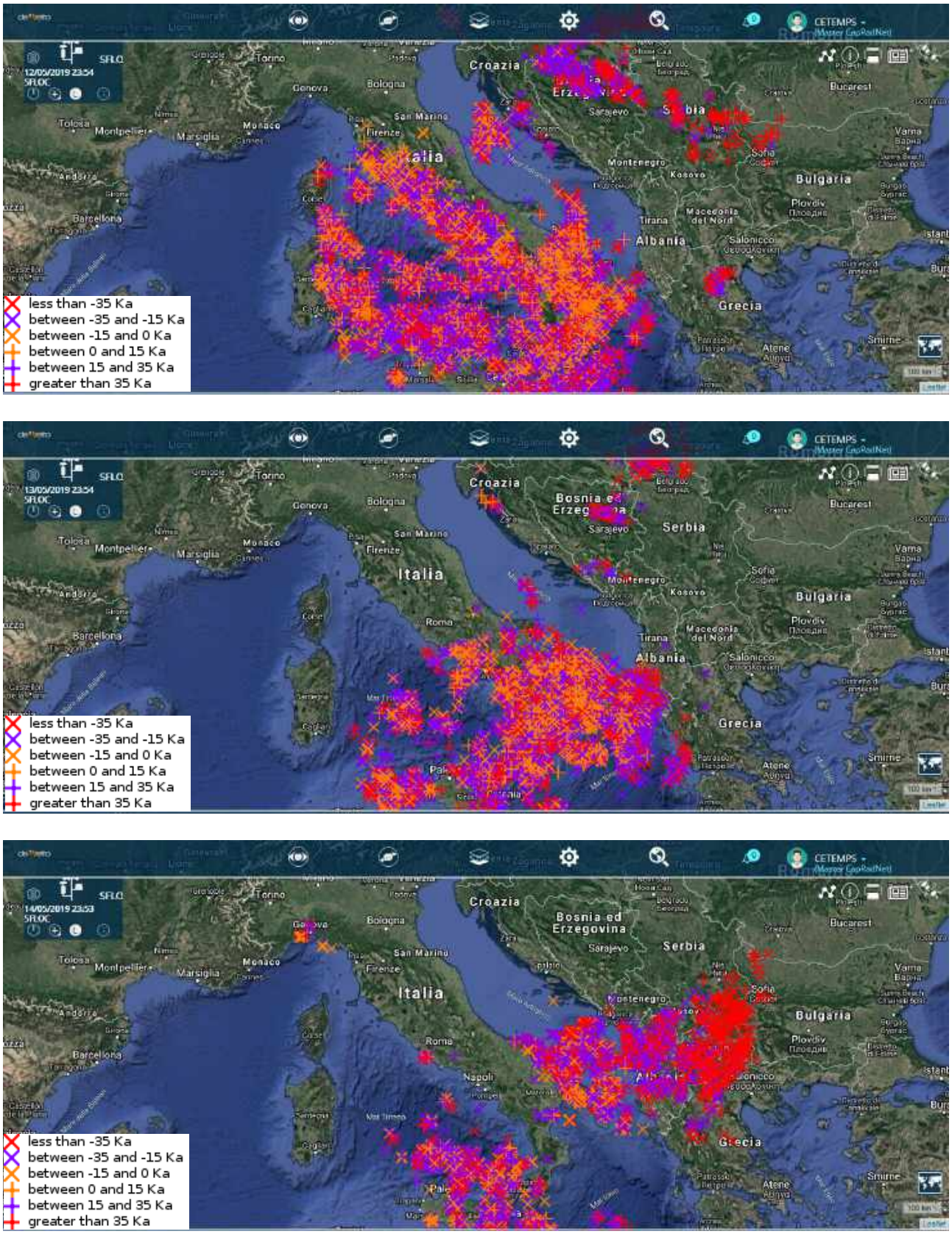

Figure 6.4.3: location and the intensity (expressed as positive or negative amperage) of the lightning strikes observed in the whole days of May 12 (top panel), 13 (central panel) and 14 (bottom panel)

7. Numerical model simulations of transport and dispersion

The primary goal of this section is to quantify river plume hydrodynamics, bed shear stress conditions, and the main pattern of biogeochemical and sedimentary tracers debouching from the Pescara River, under real field environmental conditions, i.e., flow discharge, tides, wind, and wave magnitude and direction. The simulations are based on the open source code Delft3D (http://oss.deltares.nl/web/opendelft3d), a modelling package which consists of several modules to compute amongst other the flow (FLOW), and the morphology (MOR, included in FLOW) in coastal waters. To encompass wind and wave action we also make use of a WAVE module. Below, we report details of the numerical setting we consider and the geographical domain (**figure 7.1**).

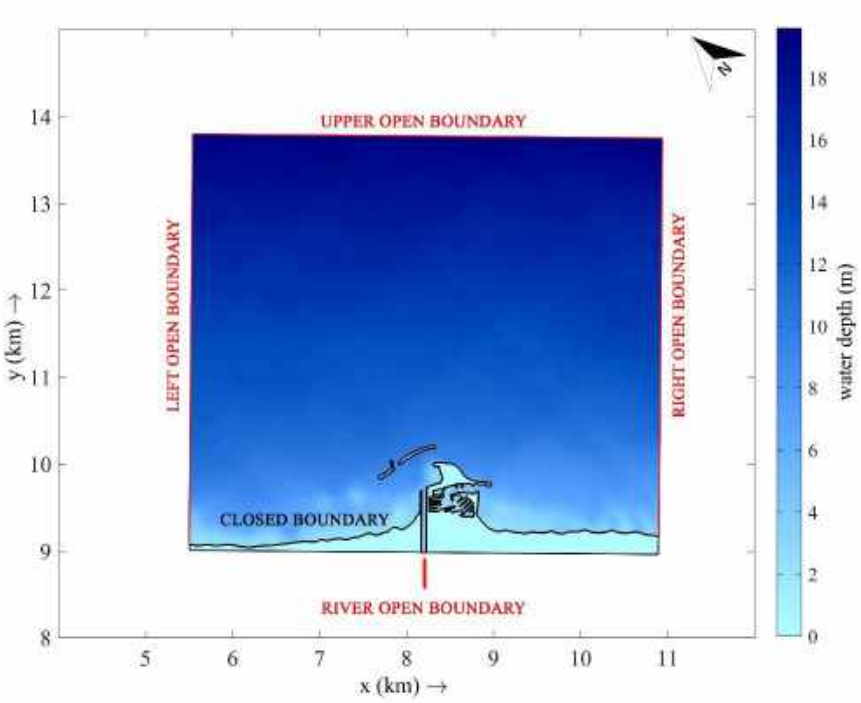

Figure 7.1: domain of the numerical runs

Flow Module

Simulation time step: 0.1 min

Grid: 902 x 802 cells

Processes: Salinity, Tracer, Sediments, Wind, Wave (online coupling.

Boundary conditions:

- Left and right open boundaries: 5 cm/s alongshore current (rightward)
- Upper boundary water level (tides provided by www.meteopesca.com)
- River Discharge (time series provided by CETEMPS)

Physical Parameters:

- Gravity 9.81 m/s^2
- Water density 1024 kg/m^3
- Air density 1 kg/m^3
- Temperature 15°C
- Roughness formula: Chezy (U=65, V=65)
- Stress formulation due to wave forces: Fredsoe
- Slip conditions: Free
- Background horizontal viscosity/diffusivity: uniform (HEV=1m^2/s, HED=10m^2/s)
- Sediment: Specific density 2650 kg/m^3, D50=0.1mm, initial sediment layer thickness: 0m; sediment flux = 0.1 kg/m^3

Wave Module

Simulation time step: 10 min (coupled online with the flow module) Grid: (351 x 301 cells)

Particle Tracking Module

Simulation time step: 0.1 min (coupled offline with the flow module) Grid: (400 x 200 cells)

Number of particles: 1000 released at the initial time of each Case (instantaneous release) within the river

Critical shear stress for sedimentation: 0.5 Pa,

Critical shear stress for erosion: 1 Pa

Settling velocity: $6x10^{-4}$ m/s

7.1 The Environmental Settings

We investigate three real-filed conditions (**figure 7.2**): i) a low river discharge case (14 July 2017), characterized by weak wind/wave conditions; ii) a high river discharge case (15 November 2017), also characterized by medium-range wind/wave conditions; iii) a medium-to-high river discharge case with a different wind/wave pattern (15 may 2019). The latter is related to the case study selected under PAI campaign and described in the previous sections.

All runs were performed by considering the Pescara outer dam in the actual conditions, and then compared with the unrealistic scenario, where no dam is present.

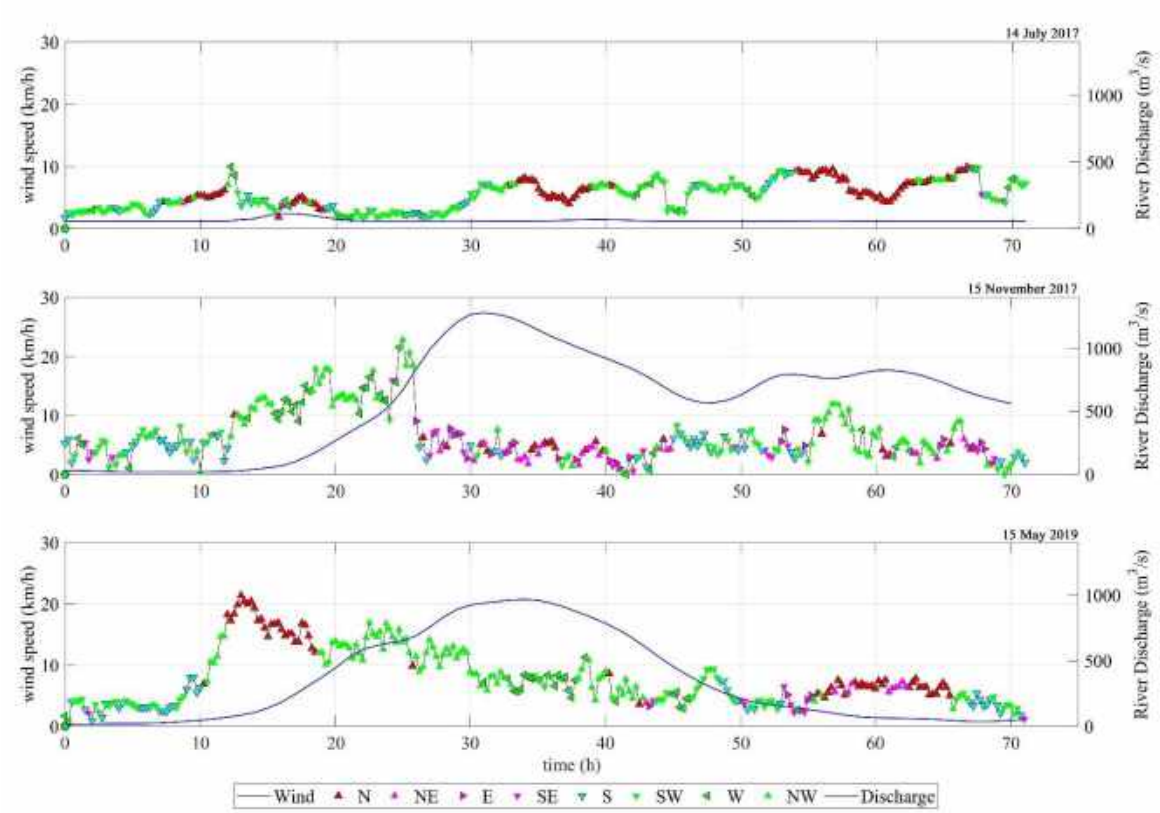

Figure 7.2: upstream environmental inputs, i.e., river discharge and wind speed, that were used for the numerical simulations of runoffs occurring on 14 July 2017 (top), 15 November 2017 (center), and 15 May 2019 (bottom)

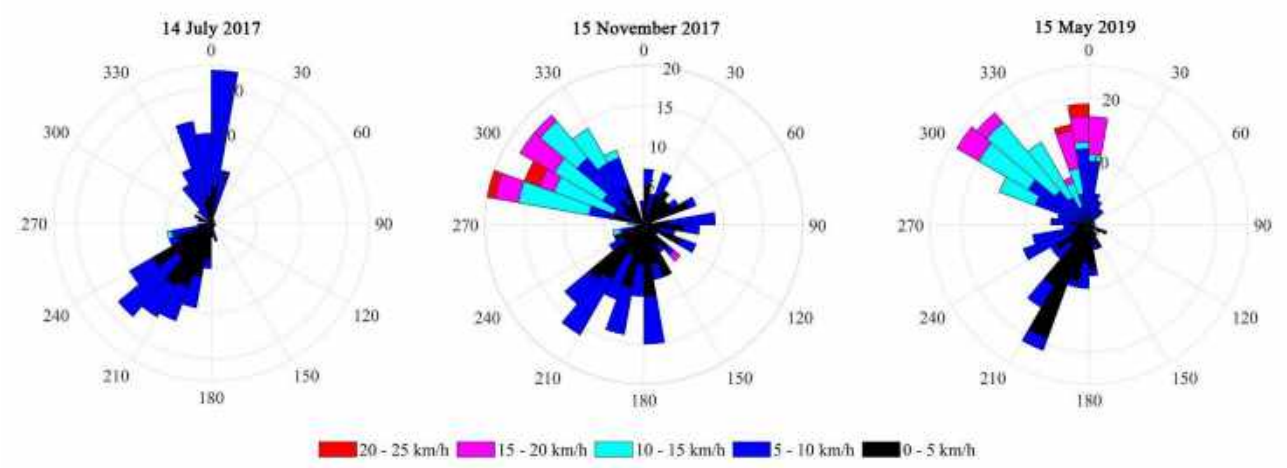

Figure 7.3: rose diagrams of the upstream winds that were used for the numerical simulations of runoffs occurring on 14 July 2017 (left), 15 November 2017 (center), and 15 May 2019 (right)

7.2 River Plume Hydrodynamics

Focusing on river plume hydrodynamics (i.e., depth averaged velocity), here we describe the case of 14 November 2017 as an representative example (**figure 7.4**), by framing the increase of river discharge from 14 hours before the flow peak (see also figure 7.2). The numerical simulation shows that the in-channel flow momentum is transferred along the north-side shoreline during the initial stage of the flood (figure 7.4; 4.10pm). This is valid for both actual dam and no dam conditions. The increase of river discharge triggers the expected anti-cyclonic circulation that characterized geophysical river plume bulges; however, for this intermediate flow stage the simulation highlights the fact that the dam significantly weakens the anti-cyclonic, southward circulation (figure 7.4; 9.10 pm). Consequently, the dam results to be responsible for a further increase of the depth averaged velocity along the northern shoreline. This behavior suddenly changes when flow discharge approaches its maximum; despite the presence of the dam, at this stage the river runoff is fully anti-cyclonic (figure 7.4; 0.30am of the 15 November 2017), as for the no dam scenario. At the maximum level of flow discharge we observe two distinct behaviors (figure 7.4; 8.50am of the 15 November 2017): the presence of the dam forces an intense southward flow of the river plume while the no dam scenario shows the classic spreading jet behavior.

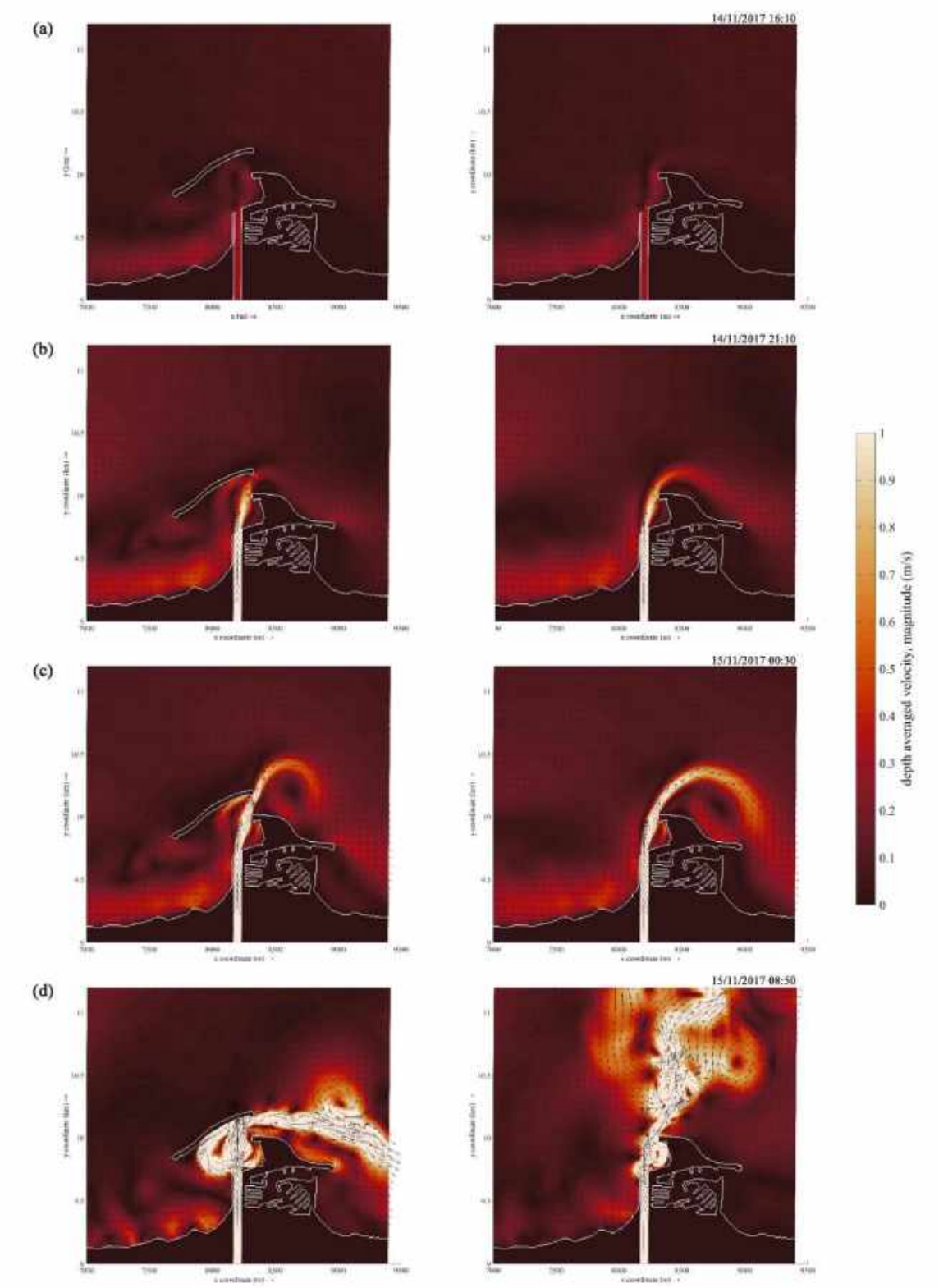

Figure 7.4: flow evolution for increasing discharge (case 14-15/11/2017); the maximum river discharge for this event is reported in the bottom panels. Left panels show the river discharge evolution (from the top to the bottom) with the actual dam condition; right panels show the no dam scenario

7.3 Analysis of Biogeochemical and Sedimentary Patterns

Here we focus on the main biogeochemical and sedimentary effects of the Pescara River runoff by analyzing passive tracer dispersion and both bed shear stress and suspended sediment distribution for each environmental conditions reported in figures 7.2 and 7.3. In particular we show patterns of: i) passive tracer concentration, which are meant to represent biogeochemical loads; ii) bed shear stress, which in turn indicates bed load transport, and iii) sedimentary deposition, superimposed with Lagrangian trajectories of sediment particles (**figures 7.5, 7.6, and 7.7**). The sediment pattern refers to the final depositional condition resulting from 70 hours since the beginning of each flood event. In particular, the sediment load released by the Pescara river is set to 0.1 kg/m^3 for the three events. Otherwise, the 1000 sediment particles used to obtain the Lagrangian trajectories are released at the very beginning of each event. All runs refer to both actual dam condition and no dam scenario and frame the resulting pattern at the end of the event.

For the low discharge event (i.e., 14 July 2017; figure 7.5), under realistic environmental conditions, passive tracers that are meant to represent biogeochemical loads, are mainly accumulated off the river mouth and delivered along the northern shoreline (figure 7.5, upper panels). This behavior does not depend on the presence of the dam; the no dam scenario shows a similar pattern to the realistic one. This is likely justified by the fact that river flow momentum is too low and, therefore, does not interact with the dam. However, the outer dam allows a relatively larger amount of the biogeochemical load to lay around the river mouth.

Things looks different from a sedimentary perspective when comparing the actual dam run with the no dam scenario. For this low river discharge case the presence of the dam causes a significant bed shear stress in front of the inner side of the dam, which mark bed load transport (figure 7.5, central panels). Although the river runoff momentum is particularly low we observe some bed shear stress along the northern side of the shoreline. Interestingly, in this region, for such relatively low flow discharge, the bed shear stress occurring during the maximum river runoff, seems to be not related to the presence of the outer dam. Sediment deposition, however, does not reach those zones that are marked by bed load transport (figure 7.5, bottom panels); a feature that indicates the lack of sedimentary balance between erosive and depositional processes.

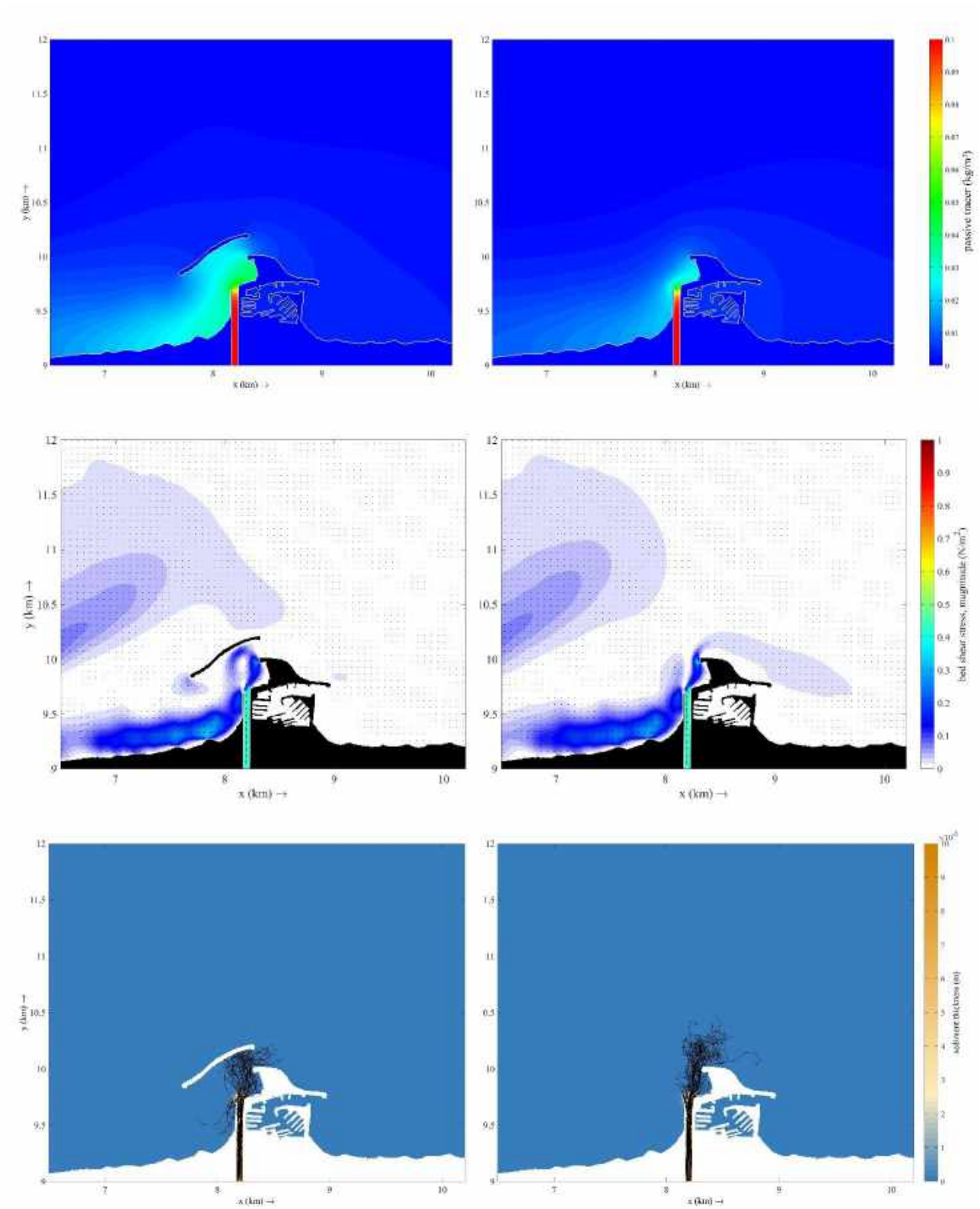

Figure 7.5: event of the 14 July 2017. Passive tracer concentration (upper panels), resulting from the whole event; bed shear stress (central panels) as recorded at the maximum level of river discharge; sedimentary deposition resulting from the whole event, superimposed with Lagrangian trajectories of sediment particles (bottom panels). Left panels refer to actual dam condition; right panels show the no dam scenario

Numerical simulations for the high river discharge event (figure 7.6; i.e., 15 November 2017) show a rather different pattern, both in terms of biogeochemical and sedimentary effects. Biogeochemical loads are indeed fully trapped by the dam and are not able to spread offshore, as for the no dam scenario (figure 7.6, upper panels); in particular, the dam seems to force the passive tracer to flow northward, along the northern part of the shoreline. Also for this case we investigate the bed shear stress pattern occurring during the maximum river discharge. In terms of bed load transport, we notice that the northern shoreline is particularly affected by high values of bed shear stress, which therefore suggests erosive processes for this part of the coast (figure 7.6, central panels). Such an erosive pattern is not evident in the no dam scenario, where high valued of bed shear stress run along the jet-like plume structure. The erosive processes that characterized the northern coast are definitely enhanced by the fact that no sedimentary deposition is recorded is this area at the end of the event (figure 7.6, bottom panels). In particular, sediment tends to accumulate off the river mouth, forming a depositional mound that extend more than 2 km offshore. We finally note that, during this event the presence of the dam, although forcing sediment accumulation at the inner side of it, also helped sedimentary processes along the southern coastal zone, where sediment deposition occurs very close to the shoreline (figure 7.6, bottom left panels).

The case of 15 May 2019 (figure 7.7) is rather similar to the previous one. The only difference is that the northernmost part of the dam is opened for about 100 m, i.e. the outer dam configuration to date. The numerical results highlight however that this detail does not dramatically affect either the flow features or the final sedimentary pattern during the flood event. Indeed, also for this case we record high values of bed shear stress along the northern side of the coastal zone, enhanced by the presence of the dam, and a sediment depositional pattern that extends offshore in the no dam scenario while is trapped by the dam, with some southward spreading (figure 7.7, central and bottom panels). The main difference we observe between the two events is in the biogeochemical pattern (figure 7.7, upper panel); here the combining effect of a medium-to-high river discharge and the wind/wave pattern (figure 7.3) tends to trap the passive tracers off the river mouth. Consequently, the presence of the dam does not significantly affect the biogeochemical dispersion for this environmental condition (figure 7.7, upper panels).

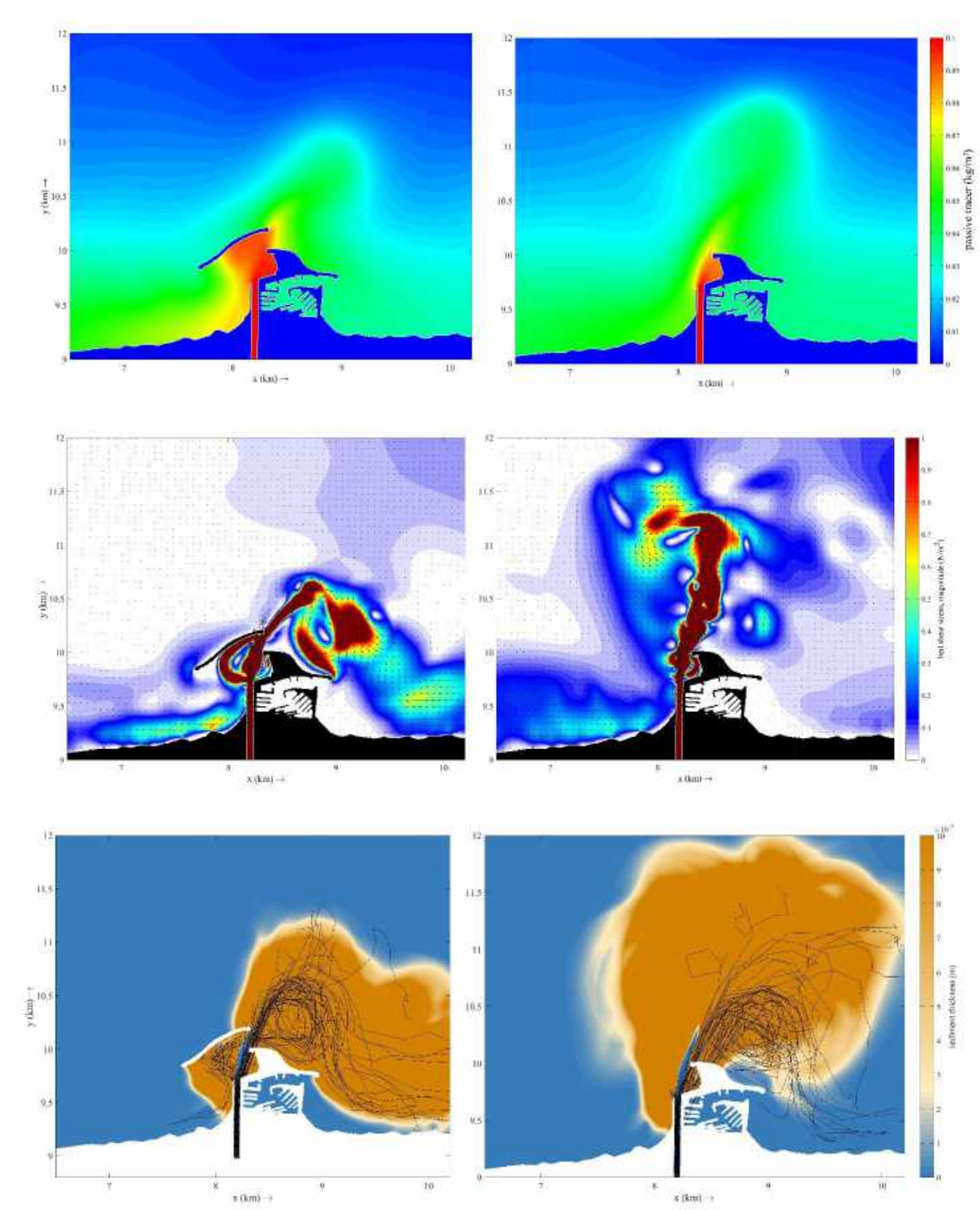

Figure 7.6: event of the 15 November 2017. Passive tracer concentration (upper panels), resulting from the whole event; bed shear stress (central panels) as recorded at the maximum level of river discharge; sedimentary deposition resulting from the whole event, superimposed with Lagrangian trajectories of sediment particles (bottom panels). Left panels refer to actual dam condition; right panels show the no dam scenario

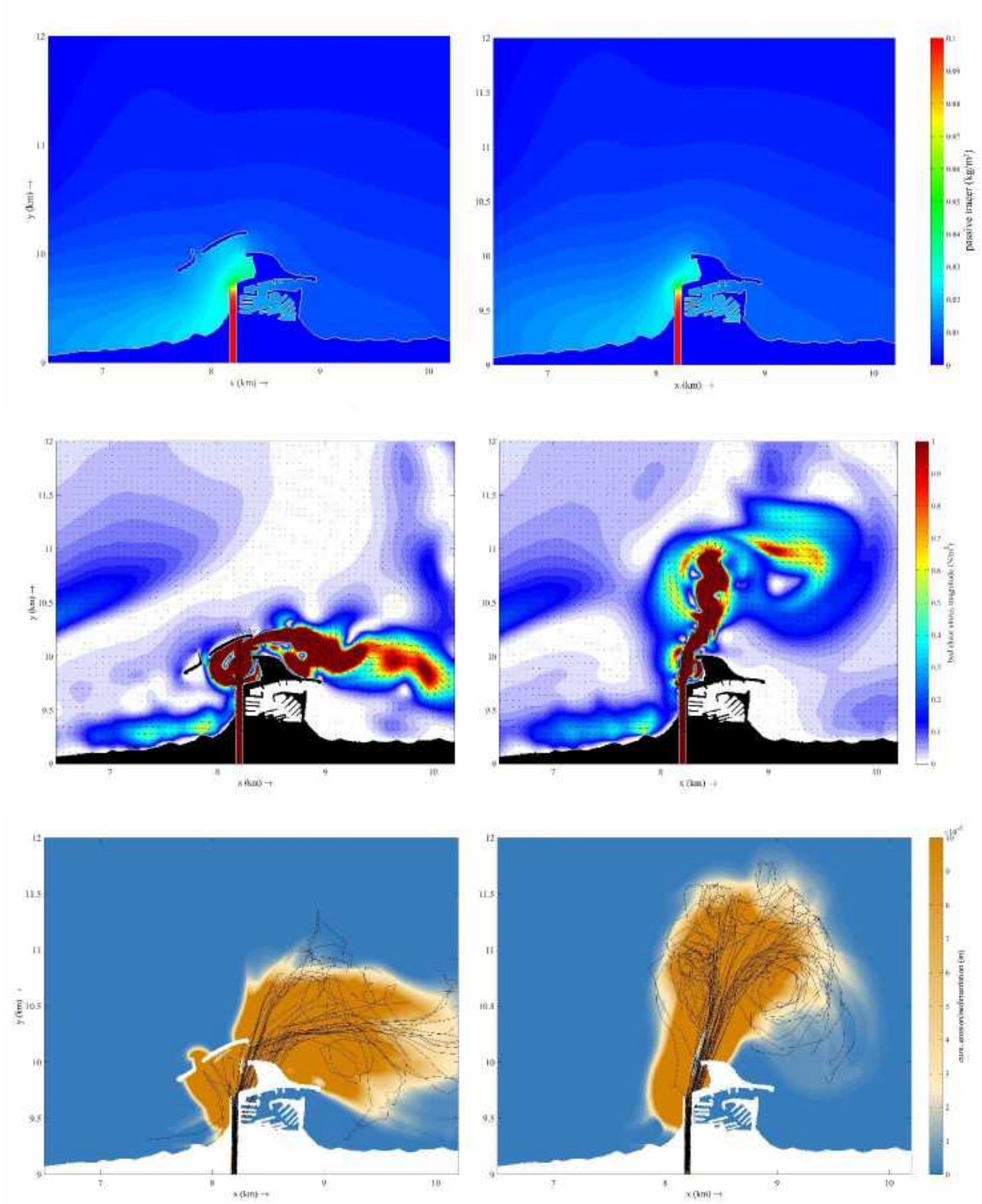

Figure 7.7: event of the 15 May 2019. Passive tracer concentration (upper panels), resulting from the whole event; bed shear stress (central panels) as recorded at the maximum level of river discharge; sedimentary deposition resulting from the whole event, superimposed with Lagrangian trajectories of sediment particles (bottom panels). Left panels refer to actual dam condition; right panels show the no dam scenario

7.4 Impacts of the Dam and Wave Action on Bed Shear Stress

To complete out analysis on the combined effect of wind/waves action and presence of the dam on bed load transport we focus on the event of the 14 November 2017. For this event, **figure 7.8** shows bed shear stress values with and without the dam, as well as with and without the river runoff action. It results that the main bed shear stress pattern off the river mouth and along the northern zone of the coast is due to the river flow action and, therefore, waves do not particularly contribute to the bed load transport during a flood. However, wave-induced bed shear stress turns to be significant (and slightly comparable with the one induced by the river runoff) along both the north and south side of the coast, far from the river mouth (figure 7.8).

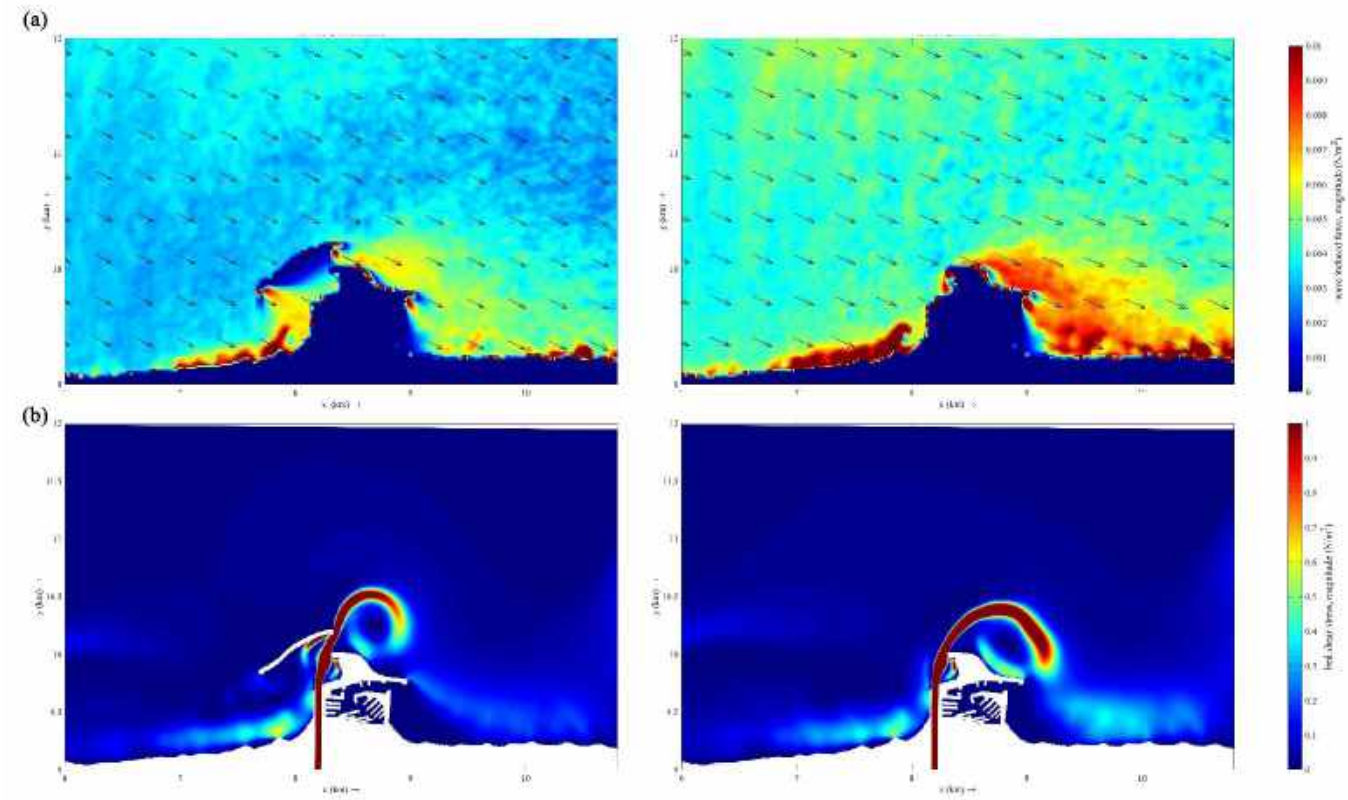

Figure 7.8: bed shear stress during the event of the 14 November 2017 (date-time: 01:10-15/11/2017) without the river flow (a) and under the action of the river flow (b). Left panels refer to the actual dam condition; right panels show the no dam scenario

7.5 Impacts of the Outer Dam on Biogeochemical and Sedimentary Pattern along the Pescara Coastal Area

Here we explore, with more details, how the presence of the dam affects both dispersion of biogeochemical tracers and sedimentary patterns due to river runoffs occurring under the three environmental conditions we consider (figure 7.2 and 7.3). In particular, we discuss the differences of i) passive tracer concentration, ii) bed shear stress, and iii) sediment deposition that result by subtracting those fields with and without the dam.

In **figure 7.9** we observe that under weak river discharge conditions (panel a) the main difference on biogeochemical tracer concentration are in the inner part of the dam and on the northern part of the coast.

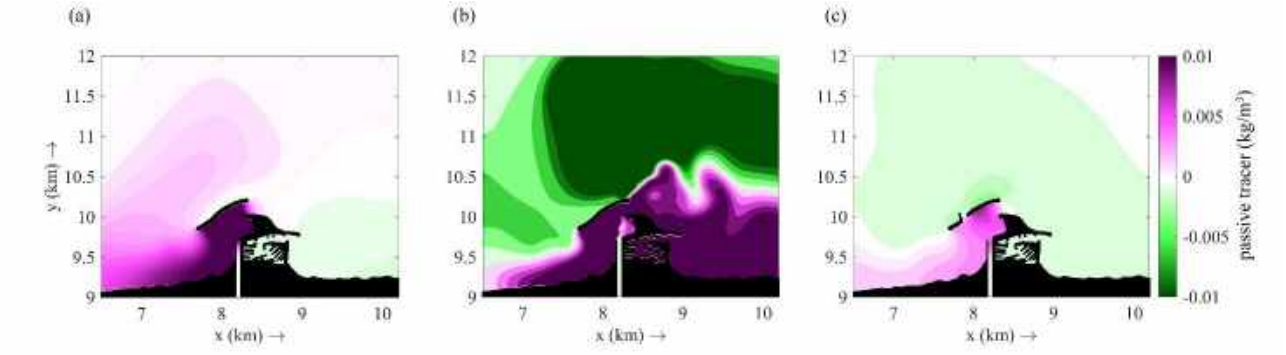

Figure 7.9: differences of passive tracers with and without the presence of the dam in its actual conditions for the three events we consider: 14 July 2017 (a), 15 November 2017 (b), and 15 May 2019 (c). Positive values refer to the simulations with the dam

We found a similar pattern in the medium-to-high river discharge conditions (panel c). This implies that under regular flow discharge (i.e., ~ 500 m^3/s) the presence of the dam significantly enhances the presence of biogeochemical tracers at the river mouth and along the northern part of the coast. On the other hand, during the intense flow discharge of 15 November 2017 (figure 7.9, panel b) the presence of the dam definitely affects the whole distribution of passive tracers in the domain. In particular, the dam enhances passive tracer concentration of both south and north side of the coast, and reduces the spreading of the tracer offshore. All this reinforce the hypotheses that the presence of the dam may dramatically affect the occurrence of biogeochemical pressures on the coastal zone, giving rise to eutrophication processes.

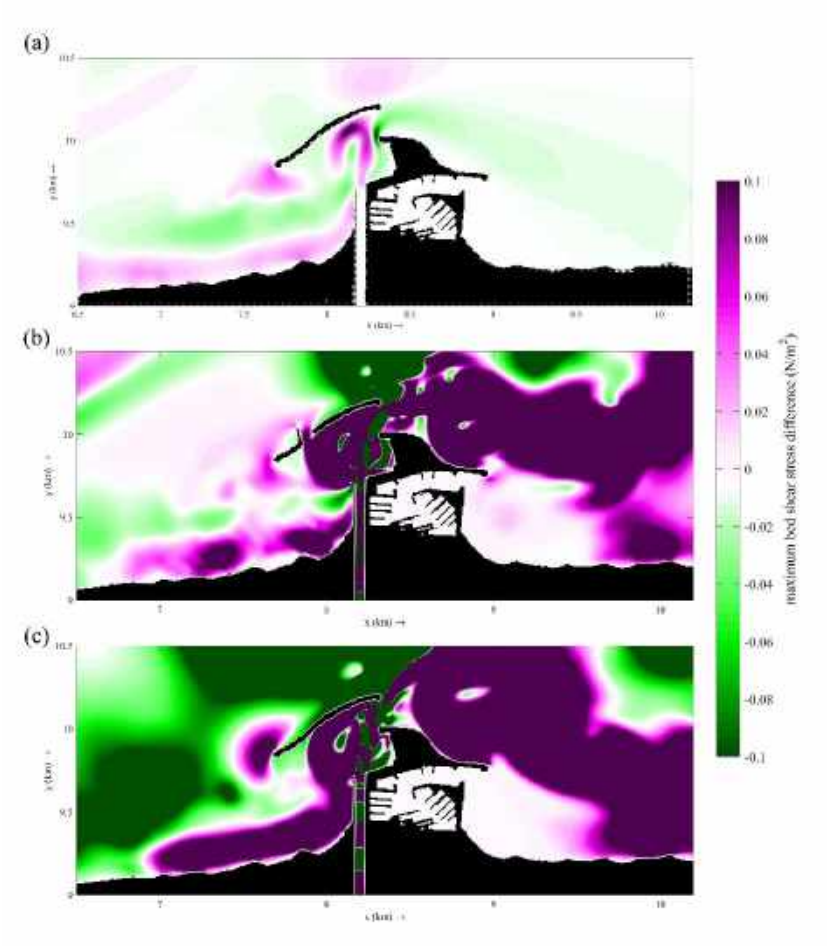

Figure 7.10: differences of bed shear stress with and without the presence of the dam in its actual conditions for the three events we consider: 14 July 2017 (a), 15 May 2019 (b) and 15 November 2017 (c). Positive values refer to the simulations with the dam

Focusing on sedimentary effects, in **figure 7.10** we show the difference of bed shear stress resulting from removing the dam in its actual conditions. As for the previous case, we consider the three environmental conditions depicted in figures 7.2 and 7.3. In general, for all the river discharge we consider, the dam enhances bed load transport along the northern coastal zone (figure 7.10). Surprisingly, this effect is more evident during the medium-to-high river discharge conditions (panel c); a feature that suggests a possible, crucial role of wind/wave pattern (north-west wind direction) in enhancing bed shear stress in this regions. Moreover, the increase of river discharge, under the effect of the dam, causes bed load transport on the southern part too (figure 7.10, panels b and c).

7.6 Concluding remarks

The numerical analysis of three different cases allows to conclude that the presence of the dam dramatically affects the flow field and the sediment pattern as a consequence of the Pescara river discharge. For river outflows of the same order of magnitude of the annual average discharge, the dam only induces a relatively larger concentration of passive tracer (i.e. biogeochemical loads) in front of the river mouth. However, the same behavior, although more pronounced, is observed also for very high flow discharges. The main differences between realistic and unrealistic condition are observed for events that are characterized by very high flow discharge, up to two order of magnitude larger than the annual average outflow. For those cases, the presence of the dam enhances the lack of sedimentary balance between erosive and depositional processes between the north side of the coast exposed to highly erosive processes and the south side of the coast, a region affected by far greater depositional contributions.